

***"This is the peer reviewed version of the following article: Straume, D., Stamsås, G. A., Berg, K. H., Salehian, Z., & Håvarstein, L. S. (2017). Identification of pneumococcal proteins that are functionally linked to penicillin-binding protein 2b (PBP2b). Molecular microbiology, 103(1), 99-116., which has been published in final form at [10.1111/mmi.13543](https://doi.org/10.1111/mmi.13543). This article may be used for non-commercial purposes in accordance with Wiley Terms and Conditions for Self-Archiving."***

1 **Identification of pneumococcal proteins that are functionally linked**  
2 **to penicillin-binding protein 2b (PBP2b).**

3 Daniel Straume, Gro Anita Stamsås, Kari Helene Berg, Zhian Salehian and Leiv Sigve Håvarstein\*

4

5 *Department of Chemistry, Biotechnology and Food Science, Norwegian University of Life*  
6 *Sciences, NO-1432 Ås, Norway.*

7

8 Running title: Identification of PBP2b accessory proteins

9 Key words: *Streptococcus pneumoniae*, elongasome, PBP2b, MreD, DivIVA, RodA

10

11

12 \* Corresponding author:

13 Leiv Sigve Håvarstein

14 Department of Chemistry, Biotechnology, and Food Science,

15 Norwegian University of Life Sciences, P.O. Box 5003, NO-1432 Ås, Norway.

16 Tlf: 47-67232493

17 Fax : 47-64965901

18 E-mail: [sigve.havarstein@nmbu.no](mailto:sigve.havarstein@nmbu.no)

19 **Summary**

20 The oval shape of pneumococci results from a combination of septal and lateral peptidoglycan  
21 synthesis. The septal cross-wall is synthesized by the divisome, while the elongasome drives cell  
22 elongation by inserting new peptidoglycan into the lateral cell wall. Each of these molecular  
23 machines contains penicillin-binding proteins (PBPs), which catalyze the final stages of  
24 peptidoglycan synthesis, plus a number of accessory proteins. Much effort has been made to  
25 identify these accessory proteins and determine their function. In the present paper we have used  
26 a novel approach to identify members of the pneumococcal elongasome that are functionally  
27 closely linked to PBP2b. We discovered that cells depleted in PBP2b, a key component of the  
28 elongasome, display several distinct phenotypic traits. We searched for proteins that, when  
29 depleted or deleted, display the same phenotypic changes. Four proteins, RodA, MreD, DivIVA  
30 and Spr0777, were identified by this approach. Together with PBP2b these proteins are essential  
31 for the normal function of the elongasome. Furthermore, our findings suggest that DivIVA, which  
32 was previously assigned as a divisomal protein, is required to correctly localize the elongasome at  
33 the negatively curved membrane region between the septal and lateral cell wall.

34

35

36

37

38

## 39 **Introduction**

40 *Streptococcus pneumoniae* is an important human pathogen with remarkable adaptation  
41 capabilities. It is a leading cause of community-acquired infections, including bacterial  
42 pneumonia, bacteremia, meningitis and otitis media. Thus, the threat of increasing  $\beta$ -lactam-  
43 resistance among pneumococci has become a major concern worldwide. Resistance to  $\beta$ -lactams  
44 in this bacterium is mediated by mosaic genes encoding altered penicillin-binding proteins (PBPs)  
45 with lower affinities for  $\beta$ -lactams than their corresponding native versions (Dowson *et al.*, 1993;  
46 Sibold *et al.*, 1994). PBPs catalyze the late steps in peptidoglycan biosynthesis, i.e. the  
47 transglycosylase and transpeptidase reactions responsible for glycan chain elongation and  
48 crosslinking, respectively (Sauvage *et al.*, 2008; Zapun *et al.*, 2008; Egan *et al.*, 2015). The  
49 resulting peptidoglycan sacculus is a giant macromolecule that provides strength to withstand  
50 turgor pressure, and serves as a scaffold for cell wall-anchored components. The construction and  
51 preservation of this structure involve a large number of enzymes, transporters and cytoskeletal  
52 elements that interact in a complex and largely unknown manner (Zapun *et al.*, 2008; Massidda *et*  
53 *al.*, 2013; Philippe *et al.*, 2014). The peptidoglycan layer consists of glycan chains composed of  
54 alternating repeats of N-acetylglucosamine (NAG) and N-acetylmuramic acid (NAM) interlinked  
55 by short peptide bridges. In *S. pneumoniae*, linear (unbranched) pentapeptides (L-alanyl- $\gamma$ -D-  
56 glutamyl-L-lysyl-D-alanyl-D-alanine) attached to NAM residues on separate glycan strands are  
57 connected by formation of a direct bond between L-lysine at position 3 on one peptide stem and  
58 D-alanine at position 4 on the other (Vollmer *et al.*, 2008). In addition to peptide bridges consisting  
59 only of cross-linked linear peptides, a considerable fraction of the bridges in pneumococcal  
60 peptidoglycan contains branched stem peptides. In branched stem peptides, a dipeptide branch  
61 consisting of L-alanine or L-serine followed invariably by L-alanine is appended to the  $\epsilon$ -amino

62 terminus of L-lysine (Vollmer *et al.*, 2008). The sequential addition of L-alanine/L-serine and L-  
63 alanine to the  $\epsilon$ -amino group of L-lysine is carried out by MurM and MurN, respectively, and takes  
64 place at the cytoplasmic side of the membrane and (Filipe *et al.*, 2000).

65 *S. pneumoniae* produces six different PBPs: PBP1a, PBP1b, PBP2a, PBP2x, PBP2b and  
66 PBP3. The three class A enzymes (PBP1a, PBP1b and PBP2a) are bifunctional, having both  
67 transpeptidase and transglycosylase activity, while the class B PBPs (PBP2x and PBP2b) are  
68 monofunctional and possess only transpeptidase activity (Sauvage *et al.*, 2008; Zapun *et al.*; 2008).  
69 In contrast to the five cell wall-synthesizing PBPs described above, the D,D-carboxypeptidase  
70 PBP3 regulates the extent of cross linking in peptidoglycan. It removes the terminal D-Ala residue  
71 from pentapeptides side chains to reduce the availability of donor stem-peptides for the  
72 transpeptidase reaction (Hakenbeck and Kohiyama, 1982; Abdullah *et al.*, 2014). Mutants in which  
73 the genes encoding PBP1a, PBP1b or PBP2a have been deleted are viable, demonstrating that  
74 individually these PBPs are not essential for growth in the laboratory. PBP1b/PBP2a and  
75 PBP1a/PBP1b double deletion mutants can also be isolated. In contrast, a PBP1a/PBP2a double  
76 deletion as well as PBP2x and PBP2b single deletions are lethal (Kell *et al.*, 1993; Paik *et al.*,  
77 1999; Berg *et al.*, 2013).

78 Pneumococci are neither rods nor cocci, but have an intermediate ovoid shape (Philippe *et*  
79 *al.*, 2014). As the shape of bacteria depends on the shape of their peptidoglycan sacculus, the  
80 morphogenesis of *S. pneumoniae* requires septal as well as lateral peptidoglycan synthesis. The  
81 former is mediated by the divisome, while the latter involves a protein complex termed the  
82 elongasome (Zapun *et al.*, 2008; Sham *et al.*, 2012; Massidda *et al.*, 2013). The composition,  
83 architecture, regulation and exact function of these molecular machines have been the subject of  
84 intense research for decades, but there still remain many unsettled questions. Recent studies have

85 shown that PBP2x is essential for formation of the septal cross wall, while PBP2b is indispensable  
86 for lateral peptidoglycan synthesis (Berg *et al.*, 2013; Land *et al.*, 2013; Peters *et al.*, 2014; Tsui  
87 *et al.*, 2014). Hence, PBP2x and PBP2b can be used as markers for the divisome and elongasome,  
88 respectively. We have previously shown that depletion of PBP2x gives rise to elongated lemon-  
89 shaped cells that struggle to divide, while PBP2b depleted cells form extremely long chains of  
90 cells that are compressed in the direction of their long axes (Berg *et al.*, 2013). Moreover, we found  
91 that the peptidoglycan of PBP2b-depleted cells has an altered stem peptide composition (Berg *et*  
92 *al.*, 2013). Recently we discovered that in addition to the above mentioned phenotypical changes,  
93 PBP2b-depleted cells become hypersensitive to the peptidoglycan hydrolase CbpD during  
94 competence (present work).

95         It is generally believed that PBP2b depends on several accessory proteins to function  
96 properly (Massidda *et al.*, 2013). We reasoned that it should be possible to identify such accessory  
97 proteins by screening for mutants with a CbpD-hypersensitive phenotype. We succeeded in  
98 identifying four proteins that, when deleted or depleted, gave rise to CbpD-hypersensitive strains,  
99 namely: RodA, MreD, DivIVA and Spr0777. In sum, our results show that together with PBP2b  
100 these proteins are essential for the normal function of the pneumococcal elongasome.

101

## 102 **Results**

### 103 ***Hypersensitivity to the peptidoglycan hydrolase CbpD in PBP2b-depleted pneumococci***

104 *S. pneumoniae* is a naturally transformable species. When induced to competence, pneumococci  
105 readily take up exogenous DNA and incorporate it into their genomes by homologous  
106 recombination. Competent pneumococci secrete a peptidoglycan hydrolase, CbpD, which kills and

107 lyses susceptible streptococci present in the same environment (Kausmally *et al.*, 2005; Johnsborg  
108 *et al.*, 2008). This predatory mechanism, called fratricide, has presumably evolved to enable  
109 competent pneumococci to capture DNA from closely related strains and species sharing the same  
110 niche. The integral membrane protein ComM, which is only produced during the competence  
111 period, protects competent cells from committing suicide (Håvarstein *et al.*, 2006). *comM* and  
112 *cbpD* belong to the early and late competence genes, respectively. Thus, transcription of the *cbpD*  
113 gene is delayed by at least 5 minutes compared to *comM*. The mechanism by which ComM protects  
114 against self-lysis is still not understood (Straume *et al.*, 2015).

115         When inducing PBP2b-depleted pneumococci to competence we discovered that they start  
116 to lyse, meaning that they are no longer able to protect themselves against CbpD even though they  
117 possess a fully functional *comM* gene. To gradually deplete the transcription of the essential *pbp2b*  
118 gene, we used a previously described depletion system called ComRS (Berg *et al.*, 2011; Berg *et*  
119 *al.*, 2013). The system consists of a synthetic 8-amino acid peptide (ComS), a transcriptional  
120 activator (ComR) and a promoter ( $P_{comX}$ ) containing a binding site for activated ComR.  $P_{comX}$  and  
121 the constitutively expressed *comR* gene were inserted into neutral sites in the pneumococcal  
122 genome. The level of expression of genes inserted behind  $P_{comX}$  can be fine-tuned by varying the  
123 concentration of ComS in the growth medium. ComS is imported into the cytoplasm by the AmiA  
124 oligopeptide permease. Once inside the cell, it binds to and activates ComR. To be able to  
125 manipulate the expression of PBP2b, a strain was constructed in which the *pbp2b* gene was placed  
126 behind the  $P_{comX}$  promoter. Next, the native *pbp2b* gene was deleted in this strain. Due to its  
127 essentiality, PBP2b was expressed ectopically from the  $P_{comX}$  promoter during the two  
128 transformation steps required to remove the native *pbp2b* gene with a so-called Janus cassette  
129 (Sung *et al.*, 2001). To examine ComM-mediated immunity in the resulting strain, SPH157 (Table

130 1), depletion of PBP2b was performed as described previously (Berg *et al.*, 2011; Berg *et al.*,  
131 2013). Briefly, a culture of SPH157 cells grown in C medium containing 0.02  $\mu\text{M}$  ComS was  
132 washed once in C medium without ComS, and then serially diluted 2-fold in the same ComS-free  
133 medium in a 96-well microplate with a clear bottom. The microplate was placed inside a Synergy  
134 H1 Hybrid reader (BioTek, Winooski, VT, USA) at 37  $^{\circ}\text{C}$ . When reaching an  $\text{OD}_{492} \sim 0.2$  the  
135 culture was induced to competence by addition of 250  $\text{ng ml}^{-1}$  of the competence stimulating  
136 peptide (CSP). In order to measure cell lysis resulting from loss of ComM-mediated protection  
137 against CbpD, the cells were grown in the presence of 2  $\mu\text{M}$  Sytox green. Sytox green is a non-  
138 toxic, membrane-impermeable dye that fluoresces 1000 times more brightly when bound to nucleic  
139 acid. Following competence induction to activate expression of ComM and CbpD, a strong  
140 increase in fluorescence was detected in PBP2b-depleted cultures (Fig. 1c). The increase in  
141 fluorescence is caused by binding of Sytox green to DNA released from disintegrated cells. As  
142 shown in Fig. 1c, a large fraction of the PBP2b-depleted cells lysed, demonstrating that they are  
143 no longer protected by ComM.

144

#### 145 ***Screening for proteins on which PBP2b is functionally dependent***

146 We reasoned that PBP2b requires the assistance of other proteins to function properly, and  
147 that deletion or depletion of such accessory proteins would give rise to the same CbpD-  
148 hypersensitive phenotype as observed for PBP2b-depleted cells. If so, this approach could be used  
149 to screen for proteins on which PBP2b is functionally dependent. Targets were selected among  
150 proteins previously reported to be involved in pneumococcal cell division and/or elongation  
151 (Massidda *et al.*, 2013; Fenton *et al.*, 2015). Genes were deleted using the Janus cassette, or  
152 depleted as described for PBP2b above. The results presented in Table 2 show that depletion of

153 RodA and Spr0777 leads to loss of ComM-mediated immunity against CbpD. When competence  
154 was induced in cultures of RodA (strain SPH354) and Spr0777 (strain SPH355) depleted cells,  
155 extensive cell lysis was observed (Fig. 1f and g). The same result was obtained with mutants in  
156 which the genes encoding MreD (strain SPH351) and DivIVA (strain SPH361) had been deleted  
157 (Table 2 and Fig. 1d and e). In contrast, no significant increase in cell lysis was observed in  
158 competence induced strains in which PBP1a, PBP2a, PBP1b, PBP2x, MreC, GpsB, FtsW, StkP,  
159 MurJ, MltG, MapZ, RodZ, FtsB, Pmp23 or Spr1357 had been deleted or depleted (Table 2). All  
160 strains that tested negative in the lysis assay were transformed with genomic DNA containing a  
161 novobiocin marker to verify that they develop the competent state when induced by CSP. In all  
162 cases the transformation efficiency was the same as that of the wild-type R6 strain (results not  
163 shown). This demonstrates that CbpD, ComM and the other competence genes are expressed  
164 normally in these strains. To verify that the strong autolytic response observed in competence-  
165 induced cells deficient in PBP2b, RodA, Spr0777, MreD or DivIVA is caused by CbpD, we deleted  
166 the *cbpD* gene in each of the strains (SPH157, SPH354, SPH355, SPH351 and SPH361) used in  
167 the experiments presented in Fig. 1. No lysis was detected when cultures of the resulting strains  
168 were induced to competence, demonstrating that the autolytic response depends on the muralytic  
169 activity of CbpD (Fig. S1). As a further control, we deleted the *comM* gene in SPH164  
170 ( $P_{comX}::pbp2x$ ), SPH344 ( $\Delta pbp1a$ ), SPH350 ( $\Delta mreC$ ) and SPH353 ( $P_{comX}::gpsB$ ), four of the strains  
171 that tested negative in the autolysis assay (see Table 2). This was done to verify that the absence  
172 of competence-induced lysis in these strains is due to an intact ComM-mediated immunity  
173 mechanism that protects the cells against CbpD. Induction of competence in the resulting *comM*-  
174 deficient strains, which were assayed in exactly the same way as their parental strains, showed that  
175 they lysed like normal  $\Delta comM$  mutants (results not shown).

176

177 ***CbpD-hypersensitive mutant strains have altered cell morphology***

178 In addition to their CbpD-hypersensitivity, PBP2b-depleted cells display other characteristic  
179 features. They form very long chains of compressed lentil-shaped cells that are unable to split their  
180 septal cross walls (Berg *et al.*, 2013 and Fig. 2). If PBP2b cannot function normally without the  
181 assistance of RodA, Spr0777, MreD or DivIVA, it would be expected that deletion or depletion of  
182 these proteins would give rise to a PBP2b-like morphology. The results shown in Fig. 2 show that  
183 this is indeed the case. The MreD (SPH351) and DivIVA (SPH361) deletion mutants, as well as  
184 the strain depleted in RodA (SPH354), exhibited a change in morphology very similar to that of  
185 PBP2b-depleted cells. Spr0777 (SPH355) depleted cells also formed long chains of cells, but their  
186 shape were not consistently lentil-shaped as a minor portion of the cells had a more elongated  
187 form. In the case of DivIVA our results are in accordance with previous studies which have  
188 reported that pneumococcal mutants lacking this protein form chains (Fadda *et al.*, 2007; Fleurie  
189 *et al.*, 2014). In the case of MreD, however, previous studies have reported that a *S. pneumoniae*  
190 R6 strain in which MreD has been deleted displays a normal morphology (Land and Winkler,  
191 2011).

192

193 ***Characterization of strains carrying mutated variants of DivIVA***

194 DivIVA proteins from Gram-positive bacteria vary in size (Oliva *et al.*, 2010). The N-terminal  
195 ~160 amino acids are relatively conserved, while the C-terminal part varies in length between  
196 species and is much less conserved. The *Bacillus subtilis* version of DivIVA consists only of the  
197 conserved part (164 aa), while the pneumococcal protein contains an additional C-terminal tail of

198 ~100 amino acids. We wondered whether this C-terminal tail might be involved in protein-protein  
199 interactions involving other members of the elongasome. Hence, we made C-terminally truncated  
200 variants of pneumococcal DivIVA, and tested the mutants carrying the truncated proteins for  
201 morphological changes and loss of ComM-mediated immunity against CbpD. No changes in  
202 morphology or CbpD-sensitivity were observed with versions of DivIVA in which the C-terminal  
203 40, 65 and 74 amino acids had been removed (Table 3). In comparison, removal of the 92 C-  
204 terminal amino acids (DivIVA- $\Delta$ 92) gave rise to cells that formed long chains. ComM-mediated  
205 immunity to CbpD, however, was mostly intact in these cells. Interestingly, removal of the 112 C-  
206 terminal amino acids of DivIVA (DivIVA- $\Delta$ 112) gave rise to long-chain pneumococci that in  
207 addition had lost immunity and become hypersensitive to CbpD. In other words, the strain  
208 expressing the DivIVA- $\Delta$ 112 protein displays the same phenotype as the  $\Delta$ DivIVA strain (Table  
209 3).

210         It has been shown previously that DivIVA, which targets negatively-curved membranes  
211 (Lenarcic *et al.*, 2009), localizes to the septal region and the poles of *S. pneumoniae* (Fadda *et al.*,  
212 2007). To determine whether DivIVA- $\Delta$ 92 and DivIVA- $\Delta$ 112 localize normally, they were tagged  
213 with green fluorescent protein (GFP) at their C-termini and examined by fluorescence microscopy.  
214 The results showed that DivIVA- $\Delta$ 92-GFP and the “wild-type” protein (DivIVA-GFP) localize to  
215 the septum and poles. The DivIVA- $\Delta$ 112-GFP protein, on the other hand, had lost the ability to  
216 target these regions, and was found to be dispersed throughout the cytoplasm (Fig. 3). Addition of  
217 the GFP-domain to wild-type DivIVA altered the morphology of the host cells. They formed  
218 chains, but not as long as the chains formed by  $\Delta$ DivIVA mutants. This demonstrates that the  
219 presence of GFP affects the function of the DivIVA protein. Nevertheless, cells expressing  
220 DivIVA-GFP, as well as the DivIVA- $\Delta$ 92-GFP protein, were still immune to CbpD when induced

221 to competence. In contrast, cells expressing DivIVA- $\Delta$ 112-GFP lysed upon competence induction,  
222 demonstrating that loss of DivIVA-localization causes loss of CbpD-immunity.

223 Phosphoproteome analyses have revealed that pneumococcal DivIVA is phosphorylated at  
224 threonine 201 by the Ser/Thr protein kinase StkP (Sun *et al.* 2010, Nováková *et al.*, 2010). To  
225 determine whether this phosphorylation affects chain length or CbpD-sensitivity we substituted  
226 T201 with an alanine or a glutamate. The former mutation removes the phosphorylation site, while  
227 the latter is a phosphomimetic mutation. The resulting strains, DivIVA<sub>T201A</sub> and DivIVA<sub>T201E</sub>,  
228 displayed wild-type morphologies, and were immune to CbpD upon competence induction (data  
229 not shown).

230

### 231 *Analysis of stem peptide composition*

232 We have previously reported that pneumococci depleted in PBP2b incorporate a considerably  
233 higher proportion of branched stem peptides in their peptidoglycan than wild-type cells, whereas  
234 depletion of PBP2x does not affect the stem peptide composition (Berg *et al.*, 2013). To determine  
235 the effect of deleting or depleting the PBP2b accessory proteins identified above, we analyzed the  
236 stem peptide composition of the  $\Delta$ DivIVA (SPH361) and  $\Delta$ MreD (SPH351) strains, and the strains  
237 depleted in RodA (SPH354) and Spr0777 (SPH355). Purified peptidoglycan from each strain was  
238 treated with LytA to release the stem peptides. To separate the peptides, the digested samples were  
239 analyzed by reversed-phase HPLC. The resulting stem peptide profiles are shown in Figure 4A.  
240 Peak I in the different panels represents a tetra-tri dimer in which L-Lys (position 3) on one peptide  
241 stem is directly linked to D-Ala (position 4) on the adjacent peptide stem (Figure 4B). Peak II, on  
242 the other hand, represents a tetra(SA)tri dimer, where L-Lys (position 3) and D-Ala (position 4)

243 are indirectly linked by a Ser-Ala interpeptide bridge (Fig. 4B). Since synthesis of a tetra(SA)tri  
244 dimer involves a branched lipid II precursor, whereas synthesis of a tetra-tri dimer does not, the  
245 ratio of material eluted in the two peaks (area peak I/ area peak II) can be used to compare the  
246 level of branched stem peptides in different mutant strains. A peak I/II ratio of 2.6 was calculated  
247 for the RH1 wild-type strain. This ratio, and the ratios given below, represent the mean of two  
248 independent experiments (see Supporting Information, Table S2). Upon depletion of PBP2b this  
249 ratio changes to 0.8, reflecting a strong increase in the incorporation of branched stem peptides.  
250 The corresponding peak ratios for RodA and Spr0777-depleted strains were 1.2 and 1.7,  
251 respectively. Thus, as for PBP2b, depletion of these proteins stimulates the incorporation of  
252 branched stem peptides. Similarly, the peptidoglycan of the  $\Delta$ MreD strain (peak ratio = 1.7)  
253 contained a significantly higher amount of branched stem peptides than the RH1 wild type strain,  
254 while the increase was more modest in the  $\Delta$ DivIVA strain (peak ratio = 2.2).

255         Analysis of peptidoglycan from cells in which ectopic PBP2b expression was driven by  
256 0.02  $\mu$ M ComS inducer revealed a peak ratio of 2.2. This is close to wild-type, but a ComS  
257 concentration of 0.02  $\mu$ M might be a bit too low to induce normal expression levels of PBP2b,  
258 resulting in a reduced peak ratio compared to wild type. However, when adding 2  $\mu$ M ComS to  
259 the growth medium to overexpress PBP2b, a peak ratio of 3.2 was obtained. It follows from this  
260 that overexpression of PBP2b leads to an increase in the relative content of unbranched stem  
261 peptides in pneumococcal peptidoglycan. In contrast to PBP2b, overexpression of RodA (2  $\mu$ M  
262 ComS inducer) strongly reduced the growth rate of the cells. We therefore reduced the ComS  
263 concentration to 0.05  $\mu$ M to obtain a roughly normal growth rate, and compared the stem peptide  
264 composition in cells grown under these conditions to RodA depleted cells (Figure 4A).  
265 Intriguingly, the peak ratio obtained with these cells was 3.2, compared to 1.2 in RodA depleted

266 cells. This result shows that supplementing the growth medium with 0.05  $\mu$ M ComS leads to  
267 overexpression of RodA, and that the level of RodA expression strongly influences the stem  
268 peptide composition in *S. pneumoniae*. In the case of Spr0777, the control strain was grown in 0.2  
269  $\mu$ M ComS. A peak ratio of 2.2 was obtained when the peptidoglycan from these cells was analyzed  
270 (Figure 4A).

271

### 272 ***Bacterial two-hybrid analysis of PBP2b, RodA, MreD, DivIVA and Spr0777 interactions***

273 The results presented above show that deletion or depletion of PBP2b, RodA, MreD, DivIVA and  
274 Spr0777 give rise to very similar phenotypic alterations with respect to three different traits. This  
275 represents strong evidence that the activity of these proteins are functionally linked. To investigate  
276 whether they are physically associated as well, we used the BACTH two-hybrid system to screen  
277 for protein-protein interactions (see Experimental Procedures). The BACTH system is based on  
278 the functional complementation of T18 and T25, two domains of the *Bordetella pertussis* adenylate  
279 cyclase (Karimova *et al.*, 1998). For each pair of proteins to be tested, one protein is fused to T18,  
280 while the other is fused to T25. The resulting fusion proteins are then coexpressed in an  
281 *Escherichia coli cya*-strain. Positive interactions restore adenylate cyclase activity and result in  
282 cAMP synthesis followed by cAMP/CAP activated expression of  $\beta$ -galactosidase. To estimate the  
283 level of  $\beta$ -galactosidase activity in *E. coli* cells expressing the fusion proteins to be tested, they are  
284 spotted on LB plates containing X-gal. The appearance of dark blue colonies indicate strong  
285 protein-protein interactions, while weaker interactions give rise to light blue colonies. White  
286 colonies indicate non-interacting proteins. Our results show that PBP2b forms a homodimer and  
287 that it interacts strongly with RodA (Fig. 5). Clear positive reactions were also obtained with *E.*

288 *coli* cells expressing combinations of T25-PBP2b/T18-DivIVA and T18-PBP2b/MreD-T25,  
289 demonstrating that PBP2b interacts with DivIVA as well as MreD. Positive, although weaker  
290 signals, were observed with cells expressing combinations of T25-PBP2b/Spr0777-T18 and  
291 Spr0777-T18/MreD-T25. Furthermore, DivIVA interacts strongly with itself and with the Spr0777  
292 protein. As negative controls we included empty plasmids (pKT25 and pUT18C) and the two  
293 protein pairs T25-PBP2b/Spr1357-T18 and T25-PBP2x/T18-RodA (Fig. 5).

294

## 295 **Discussion**

### 296 *PBP2b and its accessory proteins are essential components of the elongasome*

297 In the present study, we have searched for proteins that are functionally closely associated with  
298 PBP2b. We screened for proteins that upon deletion or depletion give rise to phenotypic alterations  
299 typical for PBP2b-depleted cells. These alterations include: i) loss of ComM-mediated immunity  
300 against the peptidoglycan hydrolase CbpD, ii) formation of long chains of longitudinally  
301 compressed cells, and iii) increased levels of branched muropeptides in the cell wall.  
302 Deletion/depletion of a number of proteins reported to be involved in septal or lateral  
303 peptidoglycan synthesis identified four proteins with the properties listed above, namely DivIVA,  
304 MreD, RodA and Spr0777. The unique phenotypic traits shared by cells depleted in PBP2b,  
305 DivIVA, MreD, RodA and Spr0777, provide strong evidence that these five proteins cooperate to  
306 build a functional elongasome.

307 To investigate whether PBP2b and its accessory proteins are in physical contact, we used  
308 the BACTH two-hybrid system. As shown in Fig. 5, PBP2b interacts strongly with RodA.  
309 Furthermore, we found significant interactions between PBP2b and MreD, and between PBP2b

310 and DivIVA. The  $\beta$ -galactosidase activity generated by the *E. coli* cells co-expressing the PBP2b  
311 and Spr0777 fusion proteins was relatively weak, but clearly above the negative controls. Hence,  
312 in sum, our results indicate that RodA, MreD, DivIVA, and probably also Spr0777, interact with  
313 PBP2b *in vivo*.

314

### 315 ***DivIVA is required for correct localization of the elongasome***

316 It is well established in the literature that MreB, MreC, MreD, RodA as well as certain  
317 PBPs are required for cell elongation in rod-shaped bacteria (Jones *et al.*, 2001; Stewart, 2005; den  
318 Blaauwen *et al.*, 2008). Individual inactivation of these proteins cause rod-shaped cells to round  
319 up and form spheroids. Ovoid bacteria like *S. pneumoniae* also elongate during growth, but to a  
320 lesser extent. Although rod-shaped and ovoid bacteria share some of the proteins required for  
321 lateral peptidoglycan synthesis, there is clearly major differences. One important difference is that  
322 MreB is absent in ovococci (Daniel and Errington, 2003; Philippe *et al.*, 2014). Members of the  
323 MreB family are actin homologues that assemble into helical filaments situated close to the inside  
324 of the cytoplasmic membrane (Jones *et al.*, 2001; van den Ent *et al.*, 2001). This cytoskeleton  
325 directs lateral peptidoglycan synthesis during growth of rod-shaped bacteria by positioning the cell  
326 wall elongation machinery. In rod-shaped cells, the machinery inserts new cell wall material  
327 throughout the cylindrical part of the cell in a helical MreB-associated pattern (den Blaauwen *et*  
328 *al.*, 2008). In contrast, the pneumococcal elongation machinery seems to be located close to the  
329 septal region. Evidence for this is based on the fact that PBP2b, a key component of this machinery,  
330 is located in the septal area (Morlot *et al.*, 2003; Land *et al.*, 2013; Tsui *et al.*, 2014). Since MreB  
331 is absent in *S. pneumoniae*, a different mechanism must operate to position the proteins involved  
332 in lateral peptidoglycan synthesis. DivIVA has previously been associated with the divisome

333 (Massidda *et al.*, 2013; Fadda *et al.*, 2007). Immunolocalization studies by Fadda *et al.* (2007)  
334 demonstrated that DivIVA localizes to the septal region as well as the poles in *S. pneumoniae*  
335 (Fadda *et al.*, 2007). This was confirmed by immunogold labeling, which revealed that DivIVA  
336 localizes to the regions of the cell with the strongest negatively curved membrane regions, i.e. the  
337 cell poles and the edge where the division septum meets the periphery of the cell (Fadda *et al.*,  
338 2007). In the present study, we used a novel approach based on shared phenotypic traits to show  
339 that DivIVA is part of the pneumococcal elongation machinery. We also discovered that DivIVA  
340 interacts strongly with Spr0777 in the BACTH two-hybrid assay, suggesting that DivIVA is  
341 recruited to the elongasome by Spr0777. Furthermore, DivIVA truncation experiments revealed  
342 that loss of elongasome function is closely associated with loss of DivIVA localization. Together,  
343 our results, and those of previous localization studies, represent strong evidence that: i) DivIVA is  
344 needed to correctly localize the pneumococcal elongation machinery, and ii) this machinery is  
345 positioned at the highly negatively curved membrane region between the septal and lateral cell  
346 wall.

347 In a recent paper, Fleurie *et al.* (2014) proposed that GpsB and DivIVA function as  
348 regulators of septal and lateral peptidoglycan synthesis in *S. pneumoniae*. According to their  
349 findings, one function of DivIVA might be to switch on lateral peptidoglycan synthesis to initiate  
350 cell elongation. Our results are not in conflict with this idea, as it is possible that DivIVA activates  
351 the cell elongation machinery by contributing to the correct assembly and localization of the  
352 elongasome. During synthesis of the septal cross wall, the divisome localizes in a ring at the  
353 leading edge of the constricting plasma membrane. Hence, the divisome and elongasome must be  
354 different entities that mostly operate at different locations in the cell. It is possible, however, that  
355 they form a single large complex at the initiation of cell division, i.e. when the septal cross wall

356 starts to form. Our model is in agreement with the findings of Tsui *et al.* (2014). They observed  
357 that, while PBP2x co-localizes with PBP2b during the early stages of cell division, PBP2x  
358 separates from PBP2b and moves to a central septal location at mid-to-late division.

359

### 360 ***PBP2b and RodA have a close functional relationship***

361 FtsW, RodA and SpoVE belong to the SEDS (shape, elongation, division and sporulation)  
362 family of integral membrane proteins (Gérard *et al.*, 2002). FtsW has been reported to be a lipid II  
363 flippase that translocates this peptidoglycan precursor across the cytoplasmic membrane  
364 (Mohammadi *et al.*, 2011). In *Escherichia coli*, FtsW is closely associated with a class B PBP  
365 termed PBP3 (FtsI), which corresponds to PBP2x in *S. pneumoniae* (Sauvage *et al.*, 2008). FtsW  
366 has been shown to co-immunoprecipitate with PBP3 *in vitro*, and to interact with PBP3 in a two-  
367 hybrid assay (Karimova *et al.*, 2005; Fraipont *et al.*, 2011). FtsW and PBP3 are both essential for  
368 septal peptidoglycan synthesis during cell division in *E. coli* (Boyle *et al.*, 1997; Pastoret *et al.*,  
369 2004). Localization of FtsW to the divisome has also been demonstrated in *B. subtilis* and *S.*  
370 *pneumoniae* (Morlot *et al.*, 2004; Gamba *et al.*, 2009; Noirclerc-Savoie *et al.*, 2013). Due to their  
371 sequence homology and topological equivalence, it is likely that FtsW and RodA have the same  
372 or similar functions in the bacterial cell (Ikeda *et al.*, 1989; Gérard *et al.*, 2002). Based on this, and  
373 other data (see below), it has been proposed that RodA is a lipid II flippase that specifically serves  
374 the cell-elongation machinery (Mohammadi *et al.*, 2011; Massidda *et al.*, 2013; Philippe *et al.*,  
375 2014). However, in two recent publications, the view that FtsW and RodA are important for lipid  
376 II translocation *in vivo* was challenged (Sham *et al.*, 2014; Meeske *et al.*, 2015). Several lines of  
377 evidence were presented suggesting that another protein, termed MurJ, is responsible for lipid II  
378 flippase activity in bacteria. MurJ-type flippases are members of the multidrug/oligosaccharidyl-

379 lipid/polysaccharide (MOP) exporter superfamily (Hvorup *et al.*, 2003). MurJ is essential in *E.*  
380 *coli*, and depletion of the protein gives rise to cell-shape defects and eventually lysis.  
381 Unexpectedly, however, deletion of all 10 MOP superfamily members present in *B. subtilis* did  
382 not alter the bacterium's growth rate or cell morphology (Fay and Dworkin, 2009; Meeske *et al.*,  
383 2015). This puzzle was solved by the discovery that a previously uncharacterized protein, Amj,  
384 can substitute for YtgP, the MurJ ortholog in *B. subtilis* (Meeske *et al.*, 2015). The genomes of *S.*  
385 *pneumoniae* and other streptococci encode a single MurJ ortholog, but lack the proposed Amj  
386 flippase (Meeske *et al.*, 2015). Interestingly, MurJ from *Streptococcus pyogenes* is able to  
387 complement *E. coli* strains depleted in endogenous MurJ (Ruiz, 2009). Hence, it is reasonable to  
388 assume that pneumococcal MurJ (Spr1383), which is 56% identical to *S. pyogenes* MurJ at the  
389 amino acid sequence level, also functions as a lipid II flippase. Depletion of MurJ in *S. pneumoniae*  
390 strain R6 gave rise to elongated and sometimes lemon-shaped cells, reminiscent of the morphology  
391 observed for FtsW-depleted cells (results not shown). This, and the fact that competence-induced  
392 MurJ-depleted cells are still immune against CbpD, show that the functions of MurJ and PBP2b  
393 are not tightly associated.

394 RodA was first identified in *E. coli* as an essential protein that affects cell morphology  
395 (Matsuzawa *et al.*, 1973). *E. coli* cells with non-functional *rodA* genes lose their characteristic rod-  
396 like shape and become spherical. Furthermore, it has been reported that RodA is required for the  
397 proper function of PBP2, a monofunctional transpeptidase essential for cell elongation and shape  
398 maintenance in *E. coli* (Ishino *et al.*, 1986). Similarly, RodA and the monofunctional  
399 transpeptidases PBP2a and PBPH are essential components of the elongation machinery in *B.*  
400 *subtilis* (Henriques *et al.*, 1998; Wei *et al.*, 2003). Thus, in the model bacteria *E. coli* and *B. subtilis*,  
401 FtsW and RodA are essential and associated with the divisome and elongasome, respectively.

402 Interestingly, in *Streptococcus thermophilus* CNRZ368 deletion of either *pbp2b* or *rodA* is not  
403 lethal. However, in both cases disruption of the genes results in increased chain length and  
404 spherical instead of ovoid cells, suggesting a close functional relationship between PBP2b and  
405 RodA (Thibessard *et al.*, 2002). We observed the same close functional relationship between RodA  
406 and the elongasome-specific transpeptidase PBP2b in *S. pneumoniae*. Depletion of pneumococcal  
407 RodA gave rise to the same phenotypical changes as depletion of PBP2b, i.e. very long chains of  
408 lentil-shaped cells, increased incorporation of branched stem peptides, and hypersensitivity to  
409 CbpD. In addition, a strong interaction between RodA and PBP2b was detected in the BACTH  
410 two-hybrid assay (Fig. 5). In contrast, depletion of pneumococcal FtsW generated elongated and  
411 irregularly shaped cells that were resistant to CbpD-mediated cell lysis when induced to  
412 competence (data not shown). In sum, these results strongly indicate that there is an intimate  
413 functional relationship between PBP2b and RodA in *S. pneumoniae*.

414         During revision of the present work, a paper by Meeske *et al.* (2016) appeared that  
415 presented strong evidence that RodA and other members of the SEDS protein family are  
416 peptidoglycan polymerases. Based on this discovery it is reasonable to assume that MurJ, rather  
417 than the SEDS proteins FtsW and RodA, is the major lipid II flippase in *S. pneumoniae*. However,  
418 at present, it cannot be ruled out that SEDS proteins are both lipid II flippases and peptidoglycan  
419 polymerases. The unexpected finding that RodA is a peptidoglycan polymerase nicely explains the  
420 tight functional relationship between RodA and PBP2b, and presumably enables PBP2b to  
421 function independently of class A PBPs.

422

423

424 ***The functions of class A and B PBPs do not seem to be closely linked***

425           In contrast to pneumococcal class B PBPs, class A PBPs can to a large extent substitute for  
426 each other. The exception is PBP1b, which cannot substitute for the concomitant loss of PBP1a  
427 and PBP2a. Unexpectedly, individual deletion of PBP1a, PBP2a or PBP1b, did not give rise to the  
428 PBP2b-specific phenotypical alterations described above. This demonstrates that PBP2b does not  
429 depend on any particular class A PBP to function normally, and supports the finding that RodA  
430 rather than a class A PBP is the peptidoglycan polymerase that operates in conjunction with PBP2b  
431 to synthesize the lateral cell wall (Meeske *et al.*, 2016). By analogy, it is likely that PBP2x and  
432 FtsW work together in the divisome to synthesize the septal cross-wall. The notion that class A  
433 and B PBPs operate independently of each other in the elongasome as well as the divisome  
434 machinery is also supported by studies demonstrating that PBP2x localizes separately from PBP1a  
435 during the later stages of cell division (Land *et al.*, 2013; Tsui *et al.*, 2014). If, as the evidence  
436 suggest, the function of class A and B PBPs are not closely linked, class A PBPs are probably part  
437 of other peptidoglycan synthesizing protein complexes. Hence, it is possible that *S. pneumoniae*  
438 contains a total of five independent peptidoglycan synthesizing machineries. Apart from the  
439 elongasome and divisome, which are built around PBP2b/RodA and PBP2x/FtsW, respectively,  
440 there could be separate machineries with partly overlapping functions for each class A PBP.  
441 Alternatively, the elongasome and divisome could contain class A as well as class B PBPs, but in  
442 separate subcomplexes. The elongasome, for instance, might consist of two subcomplexes that  
443 cooperate during lateral peptidoglycan synthesis: one built around PBP2b/RodA and the other  
444 around a class A PBP. If so, these subcomplexes probably operate in a coordinated but relatively  
445 independent manner.

446

447 ***The expression levels of PBP2b and RodA have a strong impact on the stem-peptide composition***  
448 ***of the cell wall***

449           When PBP2b is depleted in pneumococcal cells, the relative content of branched stem  
450 peptides in their peptidoglycan increases significantly compared to wild type cells. Overexpression  
451 of PBP2b (2  $\mu$ M ComS), on the other hand, produce peptidoglycan with a significantly lower  
452 relative content of branched stem peptides than wild type cells and cells grown in the presence of  
453 0.02  $\mu$ M ComS (Fig 4A; Berg *et al.*, 2013). Even though overexpression of PBP2b causes  
454 significant changes in the stem peptide composition, it seems to be well tolerated by the  
455 pneumococcal cells. The generation-time at 37  $^{\circ}$ C of exponentially growing cultures exposed to  
456 0.02 and 2  $\mu$ M ComS inducer is about 35 and 40 minutes, respectively. In comparison, the  
457 generation-time of wild-type *S. pneumoniae* R6 cells is about 35 minutes. Since PBP2b  
458 overexpression increases the ratio of unbranched to branched stem peptides, while depletion has  
459 the opposite effect, it appears that unbranched stem-peptides are the preferred substrate used in  
460 transpeptidation reactions catalyzed by PBP2b. Similarly, depletion of RodA gives rise to an  
461 increased proportion of branched stem peptides in the cell wall, while overexpression has the  
462 opposite effect. This suggests that unbranched lipid II is a better substrate for RodA than branched.  
463 In contrast to PBP2b, overexpression of RodA reduces the growth rate significantly. SPH354 cells  
464 grown in the presence of 0.05  $\mu$ M ComS have a generation time of 35-40 minutes, while it  
465 increases to 60 minutes in the presence of 2  $\mu$ M inducer peptide. It is possible that overexpression  
466 of RodA is deleterious to the cells because it leads to a strong increase in the synthesis of glycan  
467 strands, which due to the stoichiometric imbalance between RodA and PBP2b might not be  
468 incorporated correctly into the cell wall or remain unprocessed. Overexpression of PBP2b, on the

469 other hand, might be better tolerated because it primarily affects the extent of glycan strand cross-  
470 linking.

471

### 472 *Deletion of MreC and MreD give rise to very different phenotypes*

473 Land and Winkler (2011) reported that MreC and MreD are essential in *S. pneumoniae*  
474 strain D39, whereas both proteins can be deleted in the R6 strain. For this reason, they speculated  
475 that their R6 strain had acquired suppressors that compensated for the loss of MreCD. They also  
476 found that  $\Delta mreCD$ ,  $\Delta mreC$  and  $\Delta mreD$  knock-out mutants of their R6 strain grow like the parental  
477 strain and have normal cell morphology. In accordance with Land and Winkler (2011) we found  
478 that *mreC* and *mreD* can be deleted in our R6 strain. However, while the  $\Delta mreC$  mutant grew well  
479 and had normal morphology (results not shown), the  $\Delta mreD$  mutant grew very slowly and formed  
480 extremely long chains of lentil-shaped cells (see Fig. 2d). Moreover, we found that the  $\Delta mreD$   
481 mutant is hypersensitive to CbpD, while the  $\Delta mreC$  mutant is immune (Table 2). The difference  
482 in phenotype between our  $\Delta mreC$  and  $\Delta mreD$  mutant strains was unexpected as the MreCD  
483 proteins have been reported to form a complex and consequently are believed to be functionally  
484 interconnected (Philippe *et al.*, 2014). This led us to check whether MreC really is essential in the  
485 D39 strain. We got the same result as for the R6 strain, i.e. MreC is not essential in either strain.  
486 The stop codon of *mreC* overlaps with the start codon of *mreD*. Consequently, the Shine-Dalgarno  
487 (SD) sequence of the *mreD* gene is located at the 3'-end of the *mreC* gene. Thus, to avoid a polar  
488 effect on the expression of MreD, it is important not to delete the SD sequence together with the  
489 *mreC* gene. As far as we can tell, the  $\Delta mreC$  mutant constructed by Land and Winkler (2011) lacks  
490 the SD sequence in front of the downstream *mreD*. Hence, it might be that a polar effect on MreD  
491 expression is the reason they identified MreC as essential in their D39 strain. In a recent paper,

492 García-Lara *et al.* (2015) reports that a *Staphylococcus aureus*  $\Delta mreC$  mutant grows identically to  
493 the parental strain, while lack of MreD leads to growth defects and abnormal cell morphology.  
494 This is very similar to the phenotypes we observe for the pneumococcal *mreC* and *mreD* mutants.

495

#### 496 ***Spr0777-a conserved protein of unknown function***

497         Similar to MreD, Spr0777 is an integral membrane protein of unknown function. It was  
498 identified by transposon mutagenesis and high-throughput sequencing (Tn-seq analysis) as a new  
499 cell wall biogenesis factor in *S. pneumoniae* (Fenton *et al.*, 2015). Spr0777 is predicted to contain  
500 eight transmembrane segments and a large extracellular loop of about 60 amino acids. Homologs  
501 of Spr0777 are widespread among Gram-positive as well as Gram-negative bacteria, suggesting  
502 that they serve an important function (Rettner and Saier, 2010). The *ydgG* gene of *E. coli* encodes  
503 a Spr0777 homolog that, when deleted, gives rise to increased biofilm thickness in flow cells. It  
504 was proposed that YdgG controls biofilm formation by acting as a transporter of the quorum-  
505 sensing signal AI-2 (Herzberg *et al.*, 2006). Later studies, however, have cast doubt on this theory  
506 (De Araujo *et al.*, 2010; Pereira *et al.*, 2013). Our finding that depletion of Spr0777 strongly affects  
507 the stem peptide composition in pneumococci, suggests that deletion of YdgG in *E. coli* may alter  
508 biofilm formation by introducing structural changes in the cell wall or outer surface of the cells.  
509 The fact that depletion of Spr0777 gives rise to phenotypical changes very similar to those  
510 observed for PBP2b-depleted cells, shows that PBP2b depends on Spr0777 to function properly.  
511 Moreover, our finding that Spr0777 interacts strongly with DivIVA (Fig. 5) indicates that Spr0777  
512 is required for the correct subcellular localization of the elongasome. In addition, Spr0777 might  
513 be important for the spatial organization of the elongasome, or be involved in regulating its activity  
514 during the cell cycle. The genome of *S. pneumoniae* contains a homolog of Spr0777 with the same

515 topology (Spr1357). In contrast to Spr0777, Spr1357 is not essential in strain R6, and depletion of  
516 the Spr1357 protein did not generate any of the phenotypic changes characteristic of PBP2b-  
517 depleted cells.

518 A better understanding of the composition and function of the pneumococcal elongasome  
519 is not only of great academic interest, but could also have important clinical implications. The  
520 bacterial cell wall biosynthesis machinery has been, and still remains, a gold mine of potential  
521 drug targets. Hence, it is likely that increased knowledge in this field will provide new perspectives  
522 and ideas that will help researchers select the best targets for future drug development.

523

## 524 **Experimental Procedures**

525

### 526 *Cultivation and transformation of S. pneumoniae*

527 Strains of *S. pneumoniae* used in this study are listed in Table 1. *S. pneumoniae* was grown in C  
528 medium (Lacks and Hotchkiss, 1960) at 37°C. Selection for *S. pneumoniae* transformants was  
529 performed anaerobically on Todd-Hewitt agar plates containing the appropriate antibiotics at the  
530 following concentrations: kanamycin (400 µg ml<sup>-1</sup>), streptomycin (200 µg ml<sup>-1</sup>), spectinomycin  
531 (200 µg ml<sup>-1</sup>) and novobiocin (2.5 µg ml<sup>-1</sup>). When necessary, ComS inducer was added to the  
532 growth medium to drive ectopic expression of specific genes. Gene depletion experiments were  
533 done by removing the ComS inducer from the growth medium as described by Berg *et al.* (2011).

534 To construct mutant strains, DNA was introduced into the genome of *S. pneumoniae* by  
535 natural transformation. When pneumococcal cultures reached OD<sub>550</sub> = 0.05- 0.1, transforming  
536 DNA and 250 ng ml<sup>-1</sup> of synthetic competence stimulating peptide (CSP-1) were added. The

537 cultures were incubated at 37°C for 120 minutes before transformants were selected on Todd-  
538 Hewitt agar plates.

539

#### 540 ***Construction of mutants***

541 Genetic knockouts or the introduction of other mutations in the *S. pneumoniae* genome were made  
542 by transforming *S. pneumoniae* with antibiotic resistance markers or cassettes containing  
543 genetically modified target genes. The DNA cassettes were constructed by overlap extension PCR  
544 (Higuchi *et al.*, 1988) following the same protocol as described in previous publications (Berg *et*  
545 *al.*, 2013, Johnsborg *et al.*, 2008). All primers used in this work are listed in the supplementary  
546 Table S1. Briefly, to create genetic knockouts the ~1000 bp region upstream and downstream of a  
547 target gene were fused to the 5' and 3' end, respectively, of a desired antibiotic resistance gene by  
548 overlap extension PCR. This amplicon was then transformed into *S. pneumoniae* to knock out the  
549 target gene by homologous recombination. In this study the majority of mutants were created by  
550 using the Janus system (Sung *et al.*, 2001), which allows insertion and deletion of the Janus in a  
551 streptomycin resistant background. Knockout mutants were screened by PCR and all mutations  
552 that were introduced in the genome of *S. pneumoniae* were confirmed by sequencing.

553

#### 554 ***Sytox assay***

555 Cell lysis of *S. pneumoniae* cultures was monitored in real time by growing the cells in the presence  
556 of Sytox Green Nucleic Acid Stain (Invitrogen™) as previously described by Straume *et al.*,  
557 (2015). Sytox fluoresces strongly upon binding DNA when excited at 485 nm. As it is unable to  
558 cross the cytoplasmic membrane, fluorescence signal will only occur when Sytox binds to DNA

559 derived from lysed cells. Cells were grown in the presence of 2  $\mu$ M Sytox Green in 96-well  
560 Corning NBS clear-bottom plates at 37°C. OD<sub>492</sub> and light emitted at 528 nm was measured  
561 separately every 5 minutes using a Synergy H1 Hybrid Reader (BioTek). At OD<sub>492</sub> ~ 0.2 the  
562 cultures were induced to competence by adding a final concentration of 250 ng ml<sup>-1</sup> CSP.

563

#### 564 ***Scanning electron microscopy and fluorescence microscopy***

565 For SEM analysis strain SPH361 ( $\Delta$ *divIVA*), SPH351 ( $\Delta$ *mreD*) and SPH350 ( $\Delta$ *mreC*) were grown  
566 to an OD<sub>550</sub> = 0.3 and collected by centrifugation at 4000 g. Cells depleted for RodA (SPH354) or  
567 Spr0777 (SPH355) were prepared using the ComRS gene depletion system (Berg *et al.*, 2011).  
568 Gene depletion was performed by following the protocol described by Berg *et al.*, (2013), except  
569 that SPH354 was pre-grown in the presence of 0.05  $\mu$ M ComS rather than 0.02  $\mu$ M. Growth was  
570 followed spectrophotometrically, and 10 ml samples were collected when the growth rate of the  
571 *rodA*- or *spr0777*-depleted cells was severely inhibited compared to the ComS-induced control  
572 cells. The collected cells were fixed and prepared for SEM analysis as previously described by  
573 Berg *et al.*, (2013).

574 Fluorescence microscopy of DivIVA-GFP, DivIVA92-GFP and DivIVA112-GFP was  
575 done using a Zeiss LSM 700 confocal microscope. *S. pneumoniae* strains expressing the different  
576 DivIVA GFP fusions from the native P<sub>*divIVA*</sub> promoter were grown to OD<sub>550</sub> = 0.2. Cells were then  
577 withdrawn and immediately examined by fluorescence microscopy.

578

579

580 ***Purification of peptidoglycan and HPLC analysis***

581 Peptidoglycan was purified as previously described by Vollmer (2007). The material was isolated  
582 from 1-2 L cultures of exponentially growing cells ( $OD_{550} = 0.4-0.5$ ) or from gene depleted cells  
583 for which growth were severally inhibited or had stopped ( $OD_{550} = 0.3-0.5$ ). Stem peptides from  
584 2 mg of peptidoglycan were released by incubation over night with 2.5  $\mu\text{g}$  of the amidase LytA in  
585 100  $\mu\text{l}$  of 20 mM Na-phosphate buffer (pH 7.0). After LytA digestion, the enzyme was precipitated  
586 by incubating the samples at 95°C for 20 minutes. After clarifying the samples by centrifugation  
587 at 20 000  $g$  for 20 minutes, pH was adjusted to 2-3 with 20% phosphoric acid. Cell wall stem  
588 peptides were separated by HPLC using a Dionex Ultimate 3000 LC system. Peptide separation  
589 was performed by injecting 40  $\mu\text{l}$  cell wall digest into a C18 reverse phase column (Vydac 218TP  
590 C18 5  $\mu\text{m}$ , Grace Davison Discovery Sciences). The peptides were eluted using a linear 120-  
591 minutes gradient of acetonitrile from 0-15% starting with buffer A containing 0.05% trifluoroacetic  
592 acid (TFA) and finishing with buffer B containing 15% acetonitrile in 0.035% TFA. The flow-rate  
593 was kept at 0.5  $\text{ml min}^{-1}$ , and peptides were detected at 206 nm.

594

595 ***BACTH two-hybrid assay***

596 BACTH is a system developed for detecting interactions between two proteins, and is based on  
597 the principle that if one protein being fused to a T18 domain interacts with another protein being  
598 fused to a T25 domain, the T18 and T25 domains form a cAMP producing enzyme who's activity  
599 can be detected. BACTH assays were performed as described by the manufacturer (Euromedex).  
600 Plasmids containing the relevant T18/T25 fusions of *pbp2b*, *rodA*, *mreD*, *spr0777*, *divIVA*,  
601 *spr1357* and *pbp2x* were isolated from *E. coli* X1-Blue cells (See supplemental material for  
602 primers, plasmids and restriction enzymes used to construct the T18/T25 fusions). Combinations

603 of these plasmids were then co-transformed (one expressing a T18-fused protein and the other  
604 expressing a T25-fused protein) into the expression cells *E. coli* BTH101 (Euromedex).  
605 Transformants were selected on LB agar plates containing both 100  $\mu\text{g ml}^{-1}$  ampicillin and 50  $\mu\text{g}$   
606  $\text{ml}^{-1}$  kanamycin. The transformants were grown to  $\text{OD}_{600} = 0.4-0.5$  at 37 °C with shaking, before  
607 2.5  $\mu\text{l}$  of the cell culture was spotted onto LB agar plates containing 100  $\mu\text{g ml}^{-1}$  ampicillin, 50  
608  $\mu\text{g ml}^{-1}$  kanamycin, 0.5 mM IPTG (Promega) and 40  $\mu\text{g ml}^{-1}$  of X-gal (Promega). The plates were  
609 incubated over night at 30 °C, protected from light. Bacterial spots that appeared blue were  
610 regarded as a positive interaction between the two proteins fused to the T18 and T25 domains.  
611 Each protein-protein interaction experiment was repeated three times.

612

### 613 **Abbreviated Summary**

614 In the present paper we show that deletion or depletion of PBP2b, RodA, MreD, DivIVA or  
615 Spr0777 induce very similar phenotypic changes in *Streptococcus pneumoniae* strain R6,  
616 providing strong evidence that these proteins cooperate to build a functional elongasome. DivIVA  
617 targets negatively curved membranes. It is therefore likely that the function of DivIVA is to  
618 correctly localize the elongasome at the highly negatively curved membrane region between the  
619 septal and lateral cell wall.

620

621

622

623

624 **Acknowledgements**

625 We thank Hilde Raanaas Kolstad at the Imaging Centre at the Norwegian University of Life  
626 Sciences for technical assistance with the SEM analysis. The study was supported by The Research  
627 Council of Norway.

628

629 **Author Contributions**

630 (i) The conception or design of study: DS, GAS, KHB, LSH

631 (ii) The acquisition, analysis or interpretation of data: DS, GAS, KHB, ZS, LSH

632 (iii) Writing of the manuscript: DS, GAS, LSH

633

634

635 **References**

636 Abdullah, M.R., Gutiérrez-Fernández, J., Pribyl, T., Gisch, N., Saleh., M., Rohde, M., *et al.* (2014)

637 Structure of the pneumococcal L,D-carboxypeptidase DacB and pathophysiological effects

638 of disabled cell wall hydrolases DacA and DacB. *Mol Microbiol* **93**: 1183-1206.

639 Berg, K.H., Biørnstad, T.J., Straume, D., and Håvarstein, L.S. (2011) Peptide-regulated gene

640 depletion system developed for use in *Streptococcus pneumoniae*. *J Bacteriol* **193**: 5207-

641 5215.

642 Berg, K.H., Stamsås, G.A., Straume, D., and Håvarstein, L.S. (2013) Effects of low PBP2b levels  
643 on cell morphology and peptidoglycan composition in *Streptococcus pneumoniae*. J  
644 Bacteriol **195**: 4342-4354.

645 Boyle, D.S., Khattar, M.M., Addinall, S.G., Lutkenhaus, J., and Donachie, W.D. (1997) *ftsW* is an  
646 essential cell-division gene in *Escherichia coli*. Mol Microbiol **24**: 1263-1273.

647 Cato, A., Jr. and Guild, W.R. (1968) Transformation and DNA size. I. Activity of fragments of  
648 defined size and a fit to a random double cross-over model. J Mol Biol **37**: 157-178.

649 Daniel, R.A., and Errington, J. (2003) Control of cell morphogenesis in bacteria: two distinct ways  
650 to make a rod-shaped cell. Cell **113**: 767-776.

651 De Araujo, C., Balestrino, D., Roth, L., Charbonnel, N., and Forestier, C. (2010) Quorum sensing  
652 affects biofilm formation through lipopolysaccharide synthesis in *Klebsiella pneumoniae*.  
653 Res Microbiol **161**: 595-603.

654 den Blaauwen, T., de Pedro, M.A., Nguyen-Distèche, M., and Ayala, J.A. (2008) Morphogenesis  
655 of rod-shaped sacculi. FEMS Microbiol Rev **32**: 321-344.

656 Dowson, C.G., Coffey, T.J., Kell, C., and Whiley, R.A. (1993) Evolution of penicillin resistance  
657 in *Streptococcus pneumoniae*; the role of *Streptococcus mitis* in the formation of a low  
658 affinity PBP2B in *S. pneumoniae*. Mol Microbiol **9**: 635-643.

659 Egan, A.J.F., Biboy, J., van't Veer, I., Breukink, E., and Vollmer, W. (2015) Activities and  
660 regulation of peptidoglycan synthases. Phil Trans R Soc B **370**: 20150031.

661 Eldholm, V., Johnsborg, O., Haugen, K., Solheim-Ohnstad, H., and Håvarstein, L.S. (2009)  
662 Fratricide in *Streptococcus pneumoniae*: contributions and role of the cell wall hydrolases  
663 CbpD, LytA and LytC. *Microbiology* **155**: 2223-2234.

664 Fadda, D., Santona, A., D'Ulisse, V., Ghelardini, P., Ennas, M.G., Whalen, M.B., *et al.* (2007)  
665 *Streptococcus pneumoniae* DivIVA: Localization and interactions in a MinCD-free  
666 context. *J Bacteriol* **189**: 1288-1298.

667 Fay, A., and Dworkin, J. (2009) *Bacillus subtilis* homologs of MviN (MurJ), the putative  
668 *Escherichia coli* lipid II flippase, are not essential for growth. *J Bacteriol* **191**: 6020-6028.

669 Fenton, A., Bernhardt, T., and Rudner, D. (2015) Identification of new cell wall biogenesis factors  
670 in *Streptococcus pneumoniae* using Tn-Seq. *Pneumonia* **7**: 54.

671 Filipe, S.R., Pinho, M.G., and Tomasz, A. (2000) Characterization of the *murMN* operon involved  
672 in the synthesis of branched peptidoglycan peptides in *Streptococcus pneumoniae*. *J Biol*  
673 *Chem* **275**: 27768-27774.

674 Fleurie, A., Manuse, S., Zhao, C., Campo, N., Cluzel, C., Lavergne, J.P., *et al.* (2014) Interplay of  
675 the serine/threonine-kinase StkP and the paralogs DivIVA and GpsB in pneumococcal cell  
676 elongation and division. *PLoS Genet* **10**: e1004275.

677 Fraipont, C., Alexeeva, S., Wolf, B., van der Ploeg, R., Schloesser, M., den Blaauwen, T., *et al.*  
678 (2011) The integral membrane FtsW protein and peptidoglycan synthase PBP3 form a  
679 subcomplex in *Escherichia coli*. *Microbiology* **157**: 251-259.

680 Gamba, P., Veening, J.W., Saunders, N.J., Hamoen, L.W., and Daniel, R.A. (2009) Two-step  
681 assembly dynamics of the *Bacillus subtilis* divisome. *J Bacteriol* **191**: 4186-4194.

682 García-Lara, J., Weihs, F., Ma, X., Walker, L., Chaudhuri, R.R., Kasturiarachchi, J., *et al.* (2015)  
683       Supramolecular structure in the membrane of *Staphylococcus aureus*. Proc Natl Acad Sci  
684       USA **112**: 15725-15730.

685 Gérard, P., Vernet, T., and Zapun, A. (2002) Membrane topology of the *Streptococcus pneumoniae*  
686       FtsW division protein. J Bacteriol **184**: 1925-1931.

687 Hakenbeck, R., and Kohiyama, M. (1982) Purification of penicillin-binding protein 3 from  
688       *Streptococcus pneumoniae*. Eur J Biochem **127**: 231-236.

689 Herzberg, M., Kaye, I.K., Peti, W., and Wood, T.K. (2006) YdgG (TqsA) controls biofilm  
690       formation in Escherichia coli K-12 through autoinducer-2 transport. J Bacteriol **188**: 587-  
691       598.

692 Håvarstein, L.S., Martin, B., Johnsborg, O., Granadel, C., and Claverys, J.P. (2006) New insights  
693       into the pneumococcal fratricide: relationship to clumping and identification of a novel  
694       immunity factor. Mol Microbiol **59**: 1297-1307.

695 Henriques, A.O., Glaser, P., Piggot, P.J., and Moran Jr, C.P. (1998) Control of cell shape and  
696       elongation by the *rodA* gene in *Bacillus subtilis*. Mol Microbiol **28**: 235-247.

697 Higuchi, R., von Beroldingen, C.H., Sensabaugh, G.F., and Erlich, H.A. (1988) DNA-typing from  
698       single hairs. Nature **332**: 543-546.

699 Hvorup, R.N., Winnen, B., Chang, A.B., Jiang, Y., Zhou, X.F., and Saier Jr, M.H. (2003) The  
700       multidrug/oligosaccharidyl-lipid/polysaccharide (MOP) exporter superfamily. Eur J  
701       Biochem **270**: 799-813.

702 Ikeda, M., Sato, T., Wachi, M., Jung, H.K., Ishino, F., Kobayashi, Y., *et al.* (1989) Structure  
703 similarity among *Escherichia coli* FtsW and RodA proteins and *Bacillus subtilis* SpoVE  
704 protein, which function in cell division, cell elongation, and spore formation, respectively.  
705 J Bacteriol 171: 6375-6378.

706 Ishino, F., Park, W., Tomioka, S., Tamaki, S., Takase, I., Kunugita, K., *et al.* (1986) Peptidoglycan  
707 synthetic activities in membranes of *Escherichia coli* caused by overproduction of  
708 penicillin-binding protein 2 and RodA protein. J Biol Chem **261**: 7024-7031.

709 Johnsborg, O., Eldholm, V., Bjørnstad, M.L., and Håvarstein, L.S. (2008) A predatory mechanism  
710 dramatically increases the efficiency of lateral gene transfer in *Streptococcus pneumoniae*  
711 and related commensal species. Mol Microbiol **69**: 245-253.

712 Johnsborg, O., and Håvarstein, L.S. (2009) Pneumococcal LytR, a protein from the LytR-CpsA-  
713 Psr family, is essential for normal septum formation in *Streptococcus pneumoniae*. J  
714 Bacteriol **191**: 5859-5864.

715 Jones, L.J.F., Carballido-López, R., and Errington, J. (2001) Control of cell shape in bacteria:  
716 helical, actin-like filaments in *Bacillus subtilis*. Cell **104**: 913-922.

717 Karimova, G., Pidoux, J., Ullmann, A., and Ladant, D. 1998. A bacterial two-hybrid system  
718 based on a reconstituted signal transduction pathway. Proc Natl Acad Sci USA **95**:  
719 5752-5756.

720 Karimova, G., Dautin, N., and Ladant, D. (2005) Interaction network among *Escherichia coli*  
721 membrane proteins involved in cell division as revealed by bacterial two-hybrid analysis.  
722 J Bacteriol **187**: 2233-2243.

723 Kausmally, L., Johnsborg, O., Lunde, M., Knutsen, E., and Håvarstein, L.S. (2005) Choline-  
724 binding protein D (CbpD) in *Streptococcus pneumoniae* is essential from competence-  
725 induced cell lysis. J Bacteriol **187**: 4338-4345.

726 Kell, C.M., Sharma, U.K., Dowson, C.G., Town, C., Balganes, T.S., and Spratt, B. (1993)  
727 Deletion analysis of the essentiality of penicillin-binding proteins 1A, 2B, and 2X of  
728 *Streptococcus pneumoniae*. FEMS Microbiol Lett **106**: 171-175.

729 Lacks, S., and Hotchkiss, R.D. (1960) A study of the genetic material determining an enzyme in  
730 pneumococcus. Biochim Biophys Acta **39**: 508-518.

731 Land, A.D., and Winkler, M.E. (2011) The requirement for pneumococcal MreC and MreD is  
732 relieved by inactivation of the gene encoding PBP1a. J Bacteriol **193**: 4166-4179.

733 Land, A.D., Tsui, H.C.T., Kocaoglu, O., Vella, S.A., Shaw, S.L., Keen, S.K., *et al.* (2013)  
734 Requirement of essential Pbp2x and GpsB for septal ring closure in *Streptococcus*  
735 *pneumoniae* D39. Mol Microbiol **90**: 939-955.

736 Lenarcic, R., Halbedel, S., Visser, L., Shaw, M., Wu, L.J., Errington, J., *et al.* (2009) Localisation  
737 of DivIVA by targeting to negatively curved membranes. EMBO J **28**: 2272-2282.

738 Massidda, O., Novakova, L., and Vollmer, W. (2013) From models to pathogens: how much have  
739 we learned about *Streptococcus pneumoniae* cell division? Environ Microbiol **15**: 3133-  
740 3157.

741 Matsuzawa, H., Hayakawa, K., Sato, T., and Imahori, K. (1973) Characterization and genetic  
742 analysis of a mutant of *Escherichia coli* K-12 with rounded morphology. J Bacteriol **115**:  
743 436-442.

744 Meeske, A.J., Sham, L.T., Kimsey, H., Koo, B.M., Gross, C.A., Bernhardt, T.G., *et al.* (2015)  
745 MurJ and a novel lipid II flippase are required for cell wall biogenesis in *Bacillus subtilis*.  
746 Proc Natl Acad Sci USA **112**: 6437-6442.

747 Meeske, A.J., Riley, E.P., Robins, W.P., Uehara, T., Mekelanos, J.J., Kahne, D., *et al.* (2016)  
748 SEDS proteins are a widespread family of bacterial cell wall polymerases. Nature  
749 doi:10.1038/nature19331.

750 Mohammadi, T., van Dam, V., Sijbrandi, R., Vernet, T., Zapun, A., Bouhss, A., *et al.* (2011)  
751 Identification of FtsW as a transporter of lipid-linked cell wall precursors across the  
752 membrane. EMBO J **30**: 1425-1432.

753 Morlot, C., Zapun, A., Dideberg, O., and Vernet, T. (2003) Growth and division of *Streptococcus*  
754 *pneumoniae*: localization of the high molecular weight penicillin-binding proteins during  
755 the cell cycle. Mol Microbiol **50**: 845-855.

756 Morlot, C., Noirclerc-Savoye, M., Zapun, A., Dideberg, O., and Vernet, T. (2004) The D,D-  
757 carboxypeptidase PBP3 organizes the division process of *Streptococcus pneumoniae*. Mol  
758 Microbiol **51**: 1641-1648.

759 Noirclerc-Savoye, M., Lantez, V., Signor, L., Philippe, J., Vernet, T., and Zapun, A. (2013)  
760 Reconstitution of membrane protein complexes involved in pneumococcal septal cell wall  
761 assembly. PloS One **8**: e75522.

762 Nováková, L., Bezousková, S., Pompach, P., Spidlová, P., Sasková, L., Weiser, J., *et al.* (2010)  
763 Identification of multiple substrates of the StkP Ser/Thr protein kinase in *Streptococcus*  
764 *pneumoniae*. J Bacteriol **192**: 3629-3638.

765 Oliva, M.A., Halbedel, S., Freund, S.M., Dutow, P., Leonard, T.A., Veprintsev, D.B., et al. (2010)  
766 Features critical for membrane binding revealed by DivIVA crystal structure. *EMBO J* **29**:  
767 1988-2001.

768 Paik, J., Kern, I., Lurz, R., and Hakenbeck R. (1999) Mutational analysis of the *Streptococcus*  
769 *pneumoniae* bimodular class A penicillin-binding proteins. *J Bacteriol* **181**: 3852-3856.

770 Pastoret, S., Fraipont, C., den Blaauwen, T., Wolf, B., Aarsman, M.E.G., Piette, A., et al. (2004)  
771 Functional analysis of the cell division protein FtsW of *Escherichia coli*. *J Bacteriol* **186**:  
772 8370-8379.

773 Pereira, C.S., Thompson, J.A., and Xavier, K.B. (2013) AI-2-mediated signalling in bacteria.  
774 *FEMS Microbiol Rev* **37**: 156-181.

775 Peters, K., Schweizer, I., Beilharz K., Stahlmann, C., Veening, J.W., Hakenbeck, R., et al. (2014)  
776 *Streptococcus pneumoniae* PBP2x mid-cell localization requires the C-terminal PASTA  
777 domains and is essential for cell shape maintenance. *Mol Microbiol* **92**: 733-755.

778 Philippe, J., Vernet, T., and Zapun, A. (2014) The elongation of ovococci. *Microb Drug Resist*  
779 **20**: 215-221.

780 Rettner, R.E., and Saier Jr, M.H. (2010) The autoinducer-2 exporter superfamily. *J Mol Microbiol*  
781 *Biotechnol* **18**: 195-205.

782 Ruiz, N. (2009) *Streptococcus pyogenes* YtgP (Spy\_0390) complements *Escherichia coli* strains  
783 depleted of the putitative peptidoglycan flippase MurJ. *Antimicrob Agents Chemother* **53**:  
784 3604-3605.

785 Sauvage, E., Kerff, F., Terrak, M., Ayala, J.A., and Charlier, P. (2008) The penicillin-binding  
786 proteins: structure and role in peptidoglycan biosynthesis. *FEMS Microbiol Rev* **32**: 234-  
787 258.

788 Sham, L.T., Tsui, H.C.T., Land, A.D., Barendt, S.M., and Winkler, M.E. (2012) Recent advances  
789 in pneumococcal peptidoglycan biosynthesis suggest new vaccine and antimicrobial  
790 targets. *Curr Opin Microbiol* **15**: 194-203.

791 Sham, L.T., Butler, E.K., Lebar, M.D., Kahne, D., Bernhardt, T.G., and Ruiz, N. (2014) MurJ is  
792 the flippase of lipid-linked precursors for peptidoglycan biogenesis. *Science* **345**: 220-222.

793 Sibold, C., Henrichsen, J., König, A., Martin, C., Chalkley, L, and Hakenbeck, R. (1994) Mosaic  
794 *pbpX* genes of major clones of penicillin-resistant *Streptococcus pneumoniae* have evolved  
795 from *pbpX* genes of a penicillin-sensitive *Streptococcus oralis*. *Mol Microbiol* **12**: 1013-  
796 1023.

797 Stewart, G.C. (2005) Taking shape: control of bacterial cell wall biosynthesis. *Mol Microbiol* **57**:  
798 1177-1181.

799 Straume, D., Stamsås, G.A., and Håvarstein, L.S. (2015) Natural transformation and genome  
800 evolution in *Streptococcus pneumoniae*. *Infect Genet Evol* **33**: 371-380.

801 Sun, X., Ge, F., Xiao, C.L., Yin, X.F., Ge, R., Zhang, L.H., et al. (2010) Phosphoproteomic  
802 analysis reveals the multiple roles of phosphorylation in pathogenic bacterium  
803 *Streptococcus pneumoniae*. *J Proteome Res* **9**: 275-282.

804 Sung, C.K., Li, H., Claverys, J.P., and Morrison, D.A. (2001) An *rpsL* cassette, Janus, for gene  
805 replacement through negative selection in *Streptococcus pneumoniae*. *Appl Environ*  
806 *Microbiol* **67**: 5190-5196.

807 Thibessard, A., Fernandez, A., Gintz, B., Leblond-Bourget, N., and Decaris, B. (2002) Effects of  
808 *rodA* and *pbp2b* disruption on cell morphology and oxidative stress response of  
809 *Streptococcus thermophilus* CNRZ368. *J Bacteriol* **184**: 2821-2826.

810 Tsui, H.C.T., Boersma, M.J., Vella, S.A., Kocaoglu, O., Kuru, E., Peceny, J.K., *et al.* (2014) Pbp2x  
811 localizes separately from Pbp2b and other peptidoglycan synthesis proteins during later  
812 stages of cell division of *Streptococcus pneumoniae* D39. *Mol Microbiol* **94**: 21-40.

813 Tsui, H.C.T., Zheng, J.J., Magallon, A.N., Ryan, J.D., Yunck, R., Rued, B.E., *et al.* (2016)  
814 Suppression of a deletion mutation in the gene encoding essential PBP2b reveals a new  
815 lytic transglycosylase involved in peripheral peptidoglycan synthesis in *Streptococcus*  
816 *pneumoniae* D39. *Mol Microbiol* doi: 10.1111/mmi.13366.

817 van den Ent, F., Amos, L.A., and Löwe, J. (2001) Prokaryotic origin of the actin cytoskeleton.  
818 *Nature* **413**: 39-44.

819 Vollmer, W. (2007) Preparation and analysis of pneumococcal murein (peptidoglycan). In  
820 *Molecular biology of streptococci*. Hakenbeck, R., and Chhatwal, S. (eds). Norfolk, United  
821 Kingdom: Horizon Bioscience, pp. 531-536.

822 Vollmer, W., Blanot, D., and de Pedro, M.A. (2008) Peptidoglycan structure and architecture.  
823 *FEMS Microbiol Rev* **32**: 149-167.

824 Wei, Y., Havasy, T., McPherson, D.C., and Popham, D.L. (2003) Rod shape determination by the  
825 *Bacillus subtilis* class B penicillin-binding proteins encoded by *pbpA* and *pbpH*. *J Bacteriol*  
826 **185**: 4717-4726.

827 Zapun, A., Vernet, T., and Pinho, M.G. (2008) The different shapes of cocci. *FEMS Microbiol*  
828 *Rev* **32**: 345-360.

829  
830  
831  
832

833 **Table 1.** Strains used in this study.

Strain	Relevant characteristics	Source
R704	R6 derivative, $\Delta comA::ermAM$ ; Ery <sup>r</sup>	J. P. Claverys <sup>a</sup>
CP1500	Contains a novobiocin resistance gene, Nov <sup>r</sup>	(Cato & Guild, 1968)
RH1	P704, but $\Delta comA::ermAM$ , $egb::spc$ , Ery <sup>R</sup> Spc <sup>R</sup>	(Johnsberg <i>et al.</i> , 2008)
RH17	RH1 but $\Delta cbpD::Janus$ Spc <sup>r</sup> , Ery <sup>r</sup> , Kan <sup>r</sup>	(Johnsberg <i>et al.</i> , 2008)
RH420	$\Delta comM::Janus$ , Spc <sup>r</sup> , Cm <sup>r</sup> Ery <sup>r</sup> , Kan <sup>r</sup>	(Eldholm <i>et al.</i> , 2009)
RH425	R704, but streptomycin resistant, Ery <sup>r</sup> , Sm <sup>r</sup>	(Johnsberg and Håvarstein, 2009)
SPH131	$\Delta comA$ , P1::P <sub>comR</sub> ::comR, P <sub>comX</sub> ::Janus, Ery <sup>r</sup> , Kan <sup>r</sup>	(Berg <i>et al.</i> , 2011)
SPH157	$\Delta comA$ , $\Delta pbp2b_{wt}$ , but expresses <i>pbp2b</i> ectopically from P <sub>comX</sub> , Ery <sup>r</sup> , Sm <sup>r</sup>	(Berg <i>et al.</i> , 2013)
SPH164	$\Delta comA$ , $\Delta pbp2x_{wt}$ , but expresses <i>pbp2x</i> ectopically from P <sub>comX</sub> , Ery <sup>r</sup> , Sm <sup>r</sup>	(Berg <i>et al.</i> , 2013)
SPH344	$\Delta comA$ , $ssbB::luc$ , $\Delta pbp1a::Janus$ , Ery <sup>r</sup> , Cm <sup>r</sup> , Kan <sup>r</sup>	This work
SPH345	$\Delta comA$ , $ssbB::luc$ , $\Delta pbp1b::Janus$ , Ery <sup>r</sup> , Cm <sup>r</sup> , Kan <sup>r</sup>	This work
SPH346	$\Delta comA$ , $ssbB::luc$ , $\Delta pbp2a::Janus$ , Ery <sup>r</sup> , Cm <sup>r</sup> , Kan <sup>r</sup>	This work
SPH347	$\Delta comA$ , $\Delta egb$ , $hirL::lacZ$ , $\Delta stkP::Janus$ , Ery <sup>r</sup> , Kan <sup>r</sup> , Cm <sup>r</sup> , Spc <sup>r</sup>	This work
SPH348	$\Delta comA$ , $\Delta mapZ::Janus$ , Ery <sup>r</sup> , Kan <sup>r</sup>	This work
SPH349	$\Delta comA$ , $\Delta pmp23::Janus$ , Ery <sup>r</sup> , Kan <sup>r</sup>	This work
SPH350	$\Delta comA$ , $\Delta mreC$ , Ery <sup>r</sup> , Sm <sup>r</sup>	This work
SPH351	$\Delta comA$ , $\Delta mreD$ , Ery <sup>r</sup> , Sm <sup>r</sup>	This work
SPH352	$\Delta comA$ , $\Delta rodZ$ , Ery <sup>r</sup> , Sm <sup>r</sup>	This work
SPH353	$\Delta comA$ , $\Delta gpsB_{wt}$ , but expresses <i>gpsB</i> ectopically from P <sub>comX</sub> , Ery <sup>r</sup> , Sm <sup>r</sup> , Spc <sup>r</sup>	This work
SPH354	$\Delta comA$ , $\Delta rodA_{wt}$ , but expresses <i>rodA</i> ectopically from P <sub>comX</sub> , Ery <sup>r</sup> , Sm <sup>r</sup>	This work
SPH355	$\Delta comA$ , $\Delta spr0777_{wt}$ , but expresses <i>spr0777</i> ectopically from P <sub>comX</sub> , Ery <sup>r</sup> , Sm <sup>r</sup>	This work
SPH356	$\Delta comA$ , $\Delta ftsB_{wt}$ , but expresses <i>ftsB</i> ectopically from P <sub>comX</sub> , Ery <sup>r</sup> , Sm <sup>r</sup>	This work
SPH357	$\Delta comA$ , $\Delta ftsW_{wt}$ , but expresses <i>ftsW</i> ectopically from P <sub>comX</sub> , Ery <sup>r</sup> , Sm <sup>r</sup>	This work
SPH358	$\Delta comA$ , $\Delta spr1357_{wt}$ , but expresses <i>spr1357</i> ectopically from P <sub>comX</sub> , Ery <sup>r</sup> , Sm <sup>r</sup>	This work
SPH359	$\Delta comA$ , $\Delta murJ_{wt}::Janus$ , but expresses <i>murJ</i> ectopically from P <sub>comX</sub> , Ery <sup>r</sup> , Sm <sup>r</sup>	This work
SPH360	$\Delta comA$ , $\Delta mltG_{wt}$ , but expresses <i>mltG</i> ectopically from P <sub>comX</sub> , Ery <sup>r</sup> , Sm <sup>r</sup>	This work
SPH361	$\Delta comA::ermAM$ , $\Delta divIVA::Janus$ , Ery <sup>r</sup> , Kan <sup>r</sup>	This work
SPH362	Native <i>divIVA</i> is replaced with <i>divIVA<sub>T201A</sub></i> , Ery <sup>r</sup> , Sm <sup>r</sup>	This work
SPH363	Native <i>divIVA</i> is replaced with <i>divIVA<sub>T201E</sub></i> , Ery <sup>r</sup> , Sm <sup>r</sup>	This work

SPH364	Native <i>divIVA</i> is replaced with <i>divIVAΔ40</i> , Ery <sup>r</sup> , Sm <sup>r</sup>	This work
SPH365	Native <i>divIVA</i> is replaced with <i>divIVAΔ65</i> , Ery <sup>r</sup> , Sm <sup>r</sup>	This work
SPH366	Native <i>divIVA</i> is replaced with <i>divIVAΔ74</i> , Ery <sup>r</sup> , Sm <sup>r</sup>	This work
SPH367	Native <i>divIVA</i> is replaced with <i>divIVAΔ92</i> , Ery <sup>r</sup> , Sm <sup>r</sup>	This work
SPH368	Native <i>divIVA</i> is replaced with <i>divIVAΔ112</i> , Ery <sup>r</sup> , Sm <sup>r</sup>	This work
SPH369	Native <i>divIVA</i> is replaced with <i>divIVA-GFP</i> , Ery <sup>r</sup> , Sm <sup>r</sup>	This work
SPH370	Native <i>divIVA</i> is replaced with <i>divIVAΔ92-GFP</i> , Ery <sup>r</sup> , Sm <sup>r</sup>	This work
SPH371	Native <i>divIVA</i> is replaced with <i>divIVAΔ112-GFP</i> , Ery <sup>r</sup> , Sm <sup>r</sup>	This work
SPH419	$\Delta comA$ , $\Delta pbp2b_{wt}$ , but expresses <i>pbp2b</i> ectopically from $P_{comX}$ , $\Delta cbpD::Janus$ , Ery <sup>r</sup> , Sm <sup>r</sup>	This work
SPH420	$\Delta comA$ , $\Delta mreD$ , $\Delta cbpD::Janus$ , Ery <sup>r</sup> , Sm <sup>r</sup>	This work
SPH421	$\Delta comA::ermAM$ , $\Delta divIVA$ , $\Delta cbpD::Janus$ , Ery <sup>r</sup> , Kan <sup>r</sup>	This work
SPH422	$\Delta comA$ , $\Delta rodA_{wt}$ , but expresses <i>rodA</i> ectopically from $P_{comX}$ , $\Delta cbpD::Janus$ Ery <sup>r</sup> , Sm <sup>r</sup>	This work
SPH423	$\Delta comA$ , $\Delta spr0777_{wt}$ , but expresses <i>spr0777</i> ectopically from $P_{comX}$ , $\Delta cbpD::Janus$ Ery <sup>r</sup> , Sm <sup>r</sup>	This work

---

834 <sup>a</sup> Gift from Jean-Pierre Claverys.

835

836

837

838

839

840

841

842

843

844 **Table 2.** CbpD-susceptibility of strains in which proteins believed to be part of the divisome or  
 845 elongasome have been deleted or depleted.

Gene product	Function	Essential in R6	Deleted/depleted	Susceptible to CbpD <sup>1</sup>
PBP1a	Glycosyltransferase/transpeptidase, peptidoglycan synthesis	No	Deleted	No
PBP2a	Glycosyltransferase/transpeptidase, peptidoglycan synthesis	No	Deleted	No
PBP1b	Glycosyltransferase/transpeptidase, peptidoglycan synthesis	No	Deleted	No
PBP2x	Transpeptidase, septal peptidoglycan synthesis	Yes	Depleted	No
PBP2b	Transpeptidase, lateral peptidoglycan synthesis	Yes	Depleted	Yes
MreC	Unknown role in lateral peptidoglycan synthesis	No	Deleted	No
MreD	Unknown role in lateral peptidoglycan synthesis	No	Deleted	Yes
GpsB	Unknown role in peptidoglycan synthesis	No	Depleted	No
DivIVA	Unknown role in peptidoglycan synthesis	No	Deleted	Yes
FtsW	Putative peptidoglycan polymerase, septal synthesis	Yes	Depleted	No
RodA	Peptidoglycan polymerase, lateral synthesis	Yes	Depleted	Yes
StkP	Serine/threonine kinase, involved in cell division	No	Deleted	No
MurJ	Putative lipid II flippase, peptidoglycan synthesis	Yes	Depleted	No
MltG	Putative endolytic transglycosylase, potential terminase	Yes	Depleted	No
MapZ	Early division site marker	No	Deleted	No
RodZ	Unknown role in lateral peptidoglycan synthesis	No <sup>2</sup>	Deleted	No
FtsB	Unknown role in septal peptidoglycan synthesis	Yes	Depleted	No
Pmp23	Peptidoglycan hydrolase	No	Deleted	No
Spr 0777	Unknown	Yes	Depleted	Yes
Spr 1357	Unknown	No	Depleted	No

846

847 <sup>1</sup>During competence, pneumococci synthesize and secrete the peptidoglycan hydrolase CbpD,  
 848 presumably to release donor-DNA from related strains and species sharing the same niche  
 849 (Straume *et al.*, 2015). To protect themselves against CbpD, competent pneumococci express the  
 850 immunity protein, ComM, which is encoded by an early competence gene (Håvarstein *et al.*, 2006).  
 851 All mutant strains in Table 1 are competent for natural transformation, and have a functional *comM*  
 852 immunity gene. Hence, they should be resistant to CbpD when secretion of this murein hydrolase  
 853 is induced by addition of CSP. However, despite having a functional *comM* gene, some  
 854 deletion/depletion mutants become highly susceptible to CbpD.

855 <sup>2</sup>Not essential in *S. pneumoniae* strain R6, but reported to be essential in *S. pneumoniae* strain D39  
 856 (Tsui *et al.*, 2016).

857

858

859

860

861 **Table 3.** Phenotype of mutants harbouring various C-terminally truncated DivIVA proteins.

862

DivIVA <sup>a</sup>	C-terminal protein sequence <sup>b</sup>	Phenotype <sup>c</sup>	
		Long-chains	Immunity to CbpD
<b>WT</b>	-QRLKSTIESQLAIVSSDWEDILRPTATYLTQTSDEAFKEVVSEVLGEP I PAPIEEEEPIDM <u>TR</u> -QFSQAEMEELQARIEVADKELSEFEAQIKQEVETPTPVVSPQVEEEPLLIQLAQCMKNQK (262)	-	+
<b>T201A</b>	-QRLKSTIESQLAIVSSDWEDILRPTATYLTQTSDEAFKEVVSEVLGEP I PAPIEEEEPIDM <u>A</u> R-QFSQAEMEELQARIEVADKELSEFEAQIKQEVETPTPVVSPQVEEEPLLIQLAQCMKNQK (262)	-	+
<b>T201E</b>	-QRLKSTIESQLAIVSSDWEDILRPTATYLTQTSDEAFKEVVSEVLGEP I PAPIEEEEPIDM <u>E</u> R-QFSQAEMEELQARIEVADKELSEFEAQIKQEVETPTPVVSPQVEEEPLLIQLAQCMKNQK (262)	-	+
<b>Δ40</b>	-QRLKSTIESQLAIVSSDWEDILRPTATYLTQTSDEAFKEVVSEVLGEP I PAPIEEEEPIDM <u>TR</u> -QFSQAEMEELQARIEVADKE (222)	-	+
<b>Δ65</b>	-QRLKSTIESQLAIVSSDWEDILRPTATYLTQTSDEAFKEVVSEVLGEP I PAPIEEEEP (197)	-	+
<b>Δ74</b>	-QRLKSTIESQLAIVSSDWEDILRPTATYLTQTSDEAFKEVVSEVLGEP (188)	-	+
<b>Δ92</b>	-QRLKSTIESQLAIVSSDWEDILRPTATYL (170)	+	+
<b>Δ112</b>	-QRLKSTIESQ (150)	+	-
<b>ΔDivIVA</b>		+	-

863

864 <sup>a</sup> Strains carrying various DivIVA mutations. WT= wild type strain. T201A and T201E indicate  
 865 strains in which threonine at position 201 (underlined) in DivIVA has been substituted with alanine  
 866 or glutamate. Δ40-Δ112 indicate the number of amino acids removed from the C-terminal end of  
 867 DivIVA in mutant strains.

868 <sup>b</sup> The position of the last amino acids in WT and truncated DivIVA proteins is given at the end of  
 869 the sequence. The underlined threonine (201) residue has been shown to be phosphorylated by  
 870 StkP (Sun *et al.*, 2010).

871 <sup>c</sup> DivIVA deletion mutants were tested for possible changes in morphology and immunity against  
 872 the peptidoglycan hydrolase CbpD. Morphology: (-), cultures that mostly consist of diplococci  
 873 and a small fraction of chains composed of 3-5 cells. (+), cultures consisting mostly of extremely  
 874 long chains of cells (~50 >100 cells). Immunity to CbpD: (-), cultures that have lost immunity to  
 875 CbpD and consequently lyse when induced to competence by the addition of CSP. (+), cultures  
 876 that do not lyse when induced to competence.

877

878

879

880

881

## 882 **Figure Legends**

883 **Fig. 1.** DNA-release assay demonstrating CbpD-mediated autolysis in pneumococcal mutants  
884 during competence. Competent pneumococci express and secrete the peptidoglycan hydrolase  
885 CbpD, presumably to kill and lyse susceptible target cells and capture their DNA. To protect  
886 themselves against CbpD pneumococci express the ComM immunity protein, an integral  
887 membrane protein of unknown function. We discovered that pneumococcal strains deleted or  
888 depleted in PBP2b, MreD, RodA, DivIVA or Spr0777 are no longer immune to CbpD, despite  
889 having a functional *comM* gene. DNA release was measured in real time by culturing the cells in  
890 the presence of the membrane-impermeable Sytox Green Nucleic Acid Stain (Invitrogen™). Sytox  
891 Green fluoresces strongly upon binding DNA when excited at 485 nm. Competence was induced  
892 by addition of CSP (250 ng ml<sup>-1</sup>) at the time points indicated by the arrows. Results were expressed  
893 as relative fluorescence units (RFU) and were normalized according to the number of cells at each  
894 time point. Solid lines; growth curves (OD<sub>492</sub>) of wild type and mutant cultures. Dotted lines;  
895 relative fluorescence units (RFU) measured automatically every 5 min by a Synergy H1 Hybrid  
896 Reader. Panel (a), wild-type control (strain RH1); panel (b), strain RH420 ( $\Delta comM$ ); panel (c),  
897 strain SPH157 (depleted in PBP2b); panel (d), strain SPH351 ( $\Delta mreD$ ); panel (e), strain SPH361  
898 ( $\Delta divIVA$ ); panel (f), strain SPH354 (depleted in RodA); and panel (g), strain SPH355 (depleted  
899 in Spr0777). Each experiment was repeated several times with similar results.

900

901 **Fig. 2.** Scanning electron microscopy images showing the long-chain phenotype characteristic of  
902 pneumococci in which PBP2b, DivIVA, MreD, RodA, and Spr0777 have been deleted or depleted.

903 Panel (a), strain RH425 (wild-type); panel (b), strain SPH350 ( $\Delta mreC$ ); panel (c), strain SPH361  
904 ( $\Delta divIVA$ ); panel (d), strain SPH351 ( $\Delta mreD$ ); panel (e), strain SPH157 [ectopic expression of  
905 PBP2b (grown in the presence of 0.02  $\mu$ M ComS inducer)]; panel (f) strain SPH157 (depleted in  
906 PBP2b); panel (g), strain SPH354 [ectopic expression of RodA (grown in the presence of 0.05  $\mu$ M  
907 ComS inducer)]; panel (h), strain SPH354 (depleted in RodA); panel (i), strain SPH355 [ectopic  
908 expression of Spr0777 (grown in the presence of 0.2  $\mu$ M ComS inducer)] and panel (j), strain  
909 SPH355 (depleted in Spr0777). Different ComS concentrations were used for ectopic expression  
910 of PBP2b, RodA and Spr0777. This was because different expression levels of these proteins are  
911 required to give optimal growth of the respective mutant strain. Bars = 1 $\mu$ m.

912

913 **Fig. 3.** Removal of the C-terminal 112 amino acids of DivIVA causes mislocalization. Wild-type  
914 DivIVA as well as the C-terminally truncated DivIVA mutants (DivIVA- $\Delta$ 92 and DivIVA- $\Delta$ 112)  
915 were tagged with green fluorescent protein (GFP) at their C-terminal ends. The proteins were  
916 expressed from the native  $P_{divIVA}$  promoter.

917

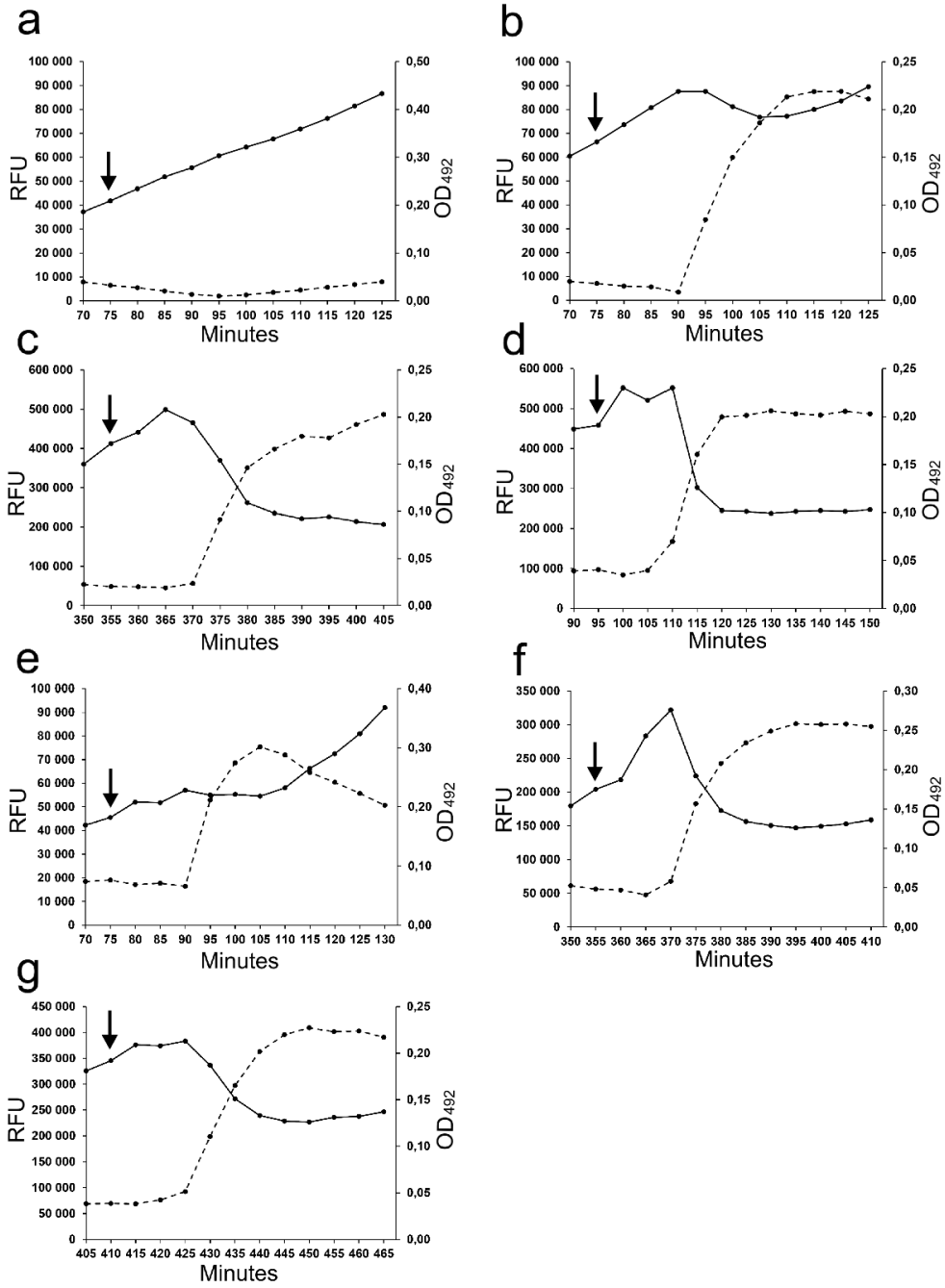
918 **Fig. 4.** Analysis of the stem peptide composition of peptidoglycan isolated from mutant strains  
919 expressing different levels of PBP2b, DivIVA, MreD, RodA and Spr0777. A. HPLC profiles of  
920 stem peptides after digesting purified peptidoglycan with LytA. PBP2b was expressed at high (2  
921  $\mu$ M ComS), intermediate (0.02  $\mu$ M ComS) and low levels (depleted). RodA and Spr0777 were  
922 expressed at low levels (depleted) and at levels that gave rise to normal cell morphology (see Fig.  
923 2). For the sake of simplicity, we compared the amount of material eluting in peak I and II, the two  
924 major peaks in the HPLC chromatogram. In a previous study (Berg *et al.*, 2013), peak I and II

925 were analyzed by mass spectrometry, and found to consist of TetraTri and Tetra(SA)Tri peptides,  
926 respectively (see panel B). The ratio between peak I and peak II was used as a measure for the  
927 content of branched stem peptides in the peptidoglycan of the mutant strains under study. The stem  
928 peptide composition analyses were repeated two times with similar results.

929

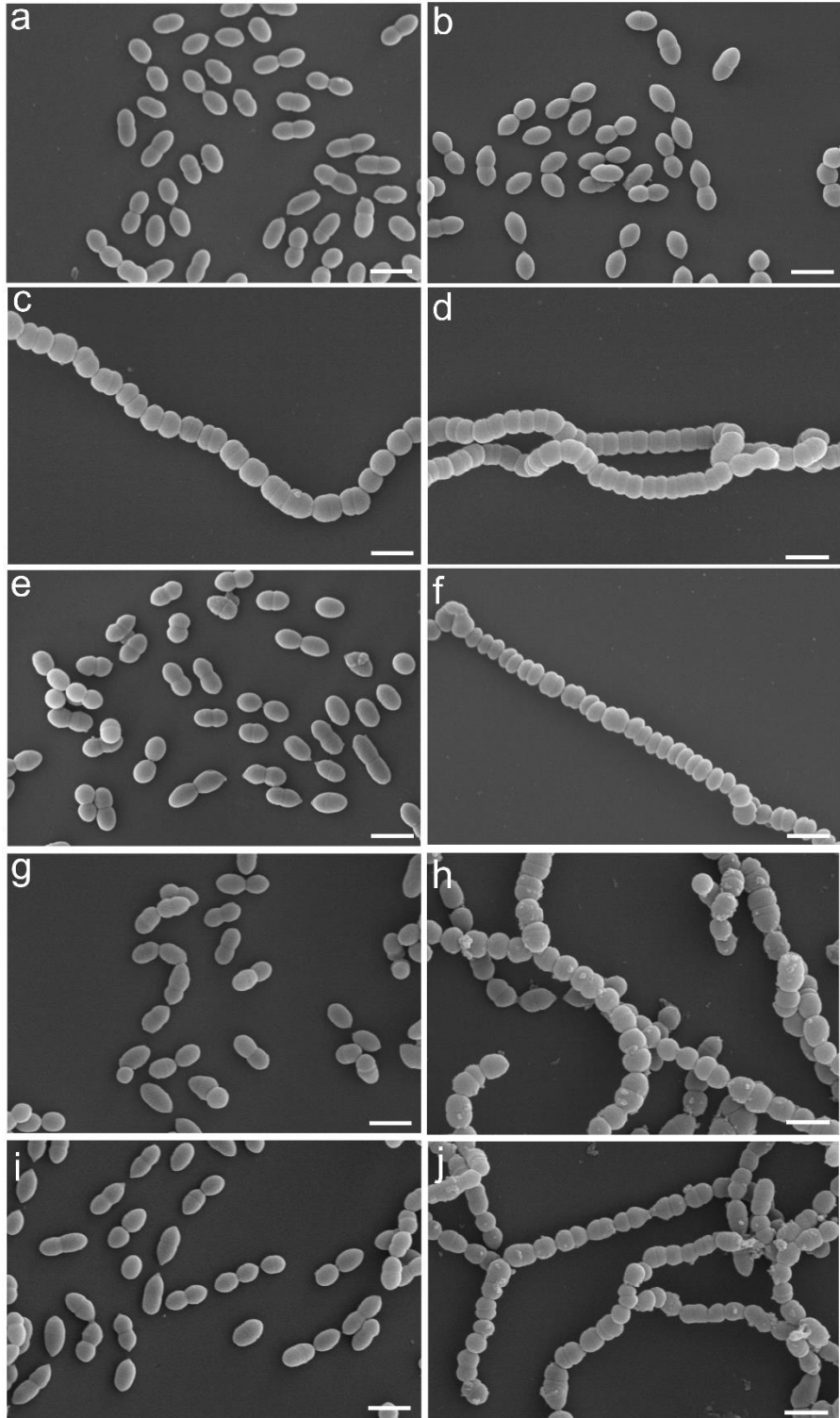
930 **Fig. 5.** Interactions between the PBP2b, DivIVA, MreD, RodA and Spr0777 proteins detected by  
931 a bacterial two-hybrid approach. An *Escherichia coli cya<sup>-</sup>* strain was co-transformed with plasmids  
932 containing the indicated fusions to adenylate cyclase fragments T18 and T25. Samples were  
933 spotted on agar plates containing X-gal and incubated for 24 hour at 30 °C. A blue colour indicates  
934 a positive interaction between the pair of fusion proteins tested, while a colourless spot indicates  
935 a negative result. Plasmids used for the positive and negative controls were supplied by  
936 Euromedex. The T25-PBP2b/Spr1357-T18 and T25-PBP2x/T18-RodA fusion pairs were included  
937 as examples of negative reactions.

938



939

940 **Fig. 1.**



941

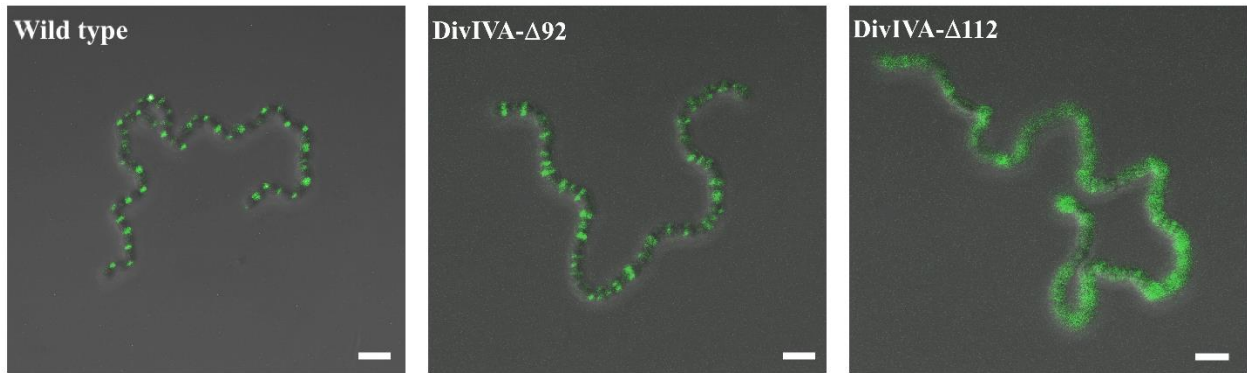
942 **Fig. 2.**

943

944

945

946

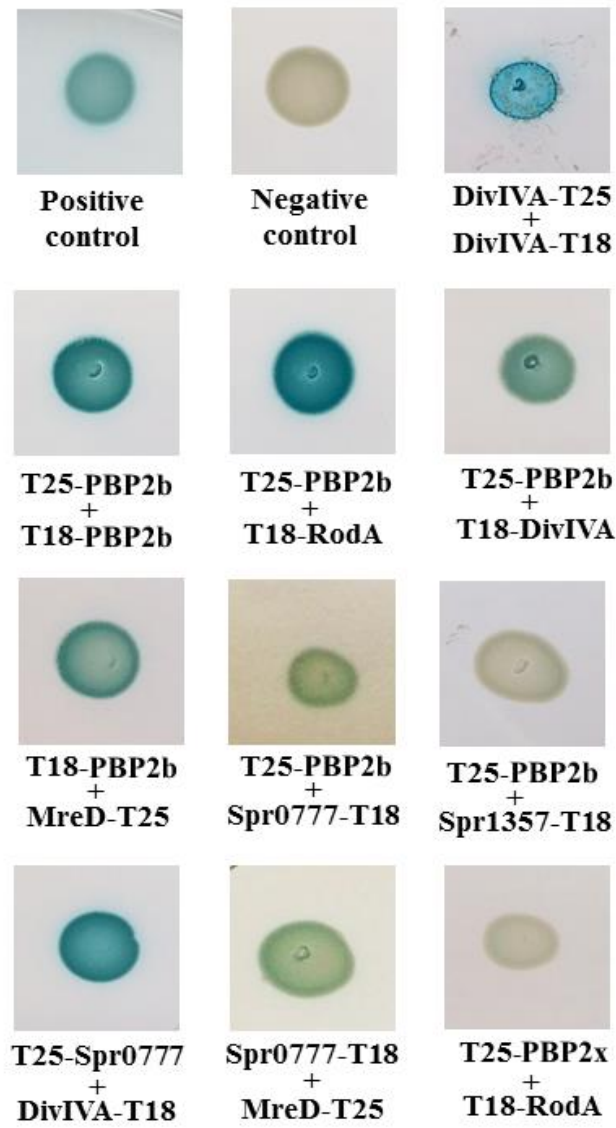


947

948 **Fig. 3.**



951



952

953

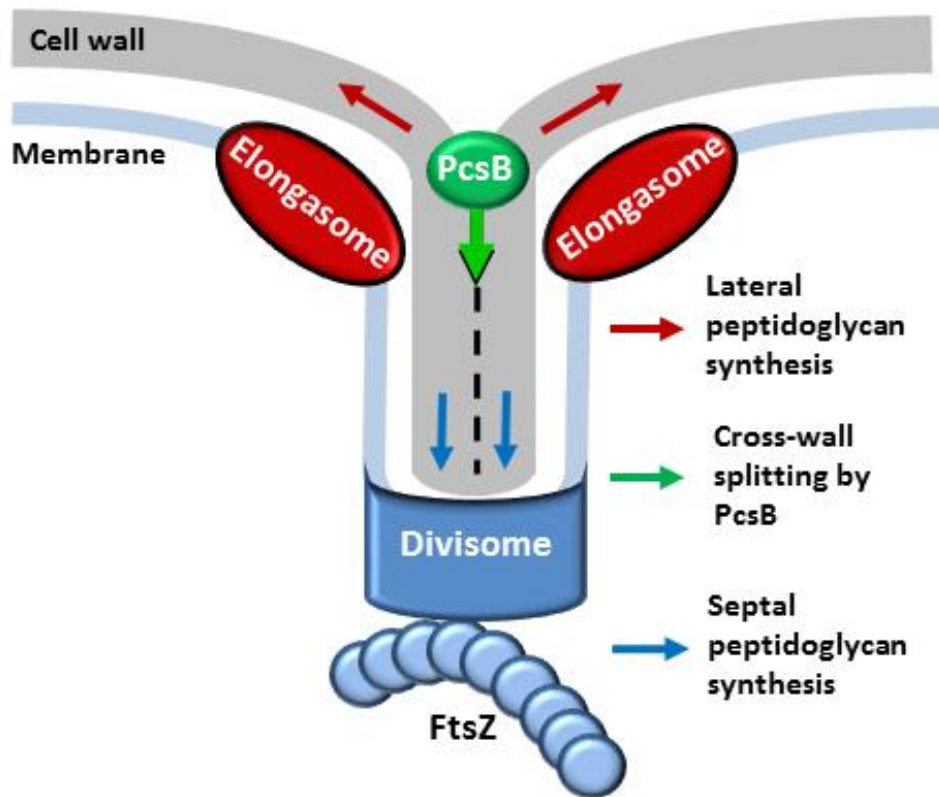
954 **Fig. 5**

955

956

957 **Graphical Abstract**

958



959

960

961

962

963

964

965

966 **Supporting Information**

967 **Table S1.** Oligonucleotide primer sequences

Name	Sequence (5' → 3')	Reference
<b>Primers used to amplify Janus</b>		
Kan484.F	GTTTGATTTTTAATGGATAATGTG	(Johnsborg <i>et al.</i> , 2008)
RpsL41.R	CTTTCCTTATGCTTTTTGGAC	(Johnsborg <i>et al.</i> , 2008)
khh94	AAGTATTTTCTAGTATTATAGCACATTTAACTTTCCTTATGCTTTTTG GAC	This work
<b>Primers used to amplify <math>P_{comX}</math> and the <math>\Delta P_{comX}</math>::Janus amplicon</b>		
khh31	ATAACAAATCCAGTAGCTTTGG	(Berg <i>et al.</i> , 2011)
khh33	TTTCTAATATGTAACCTTCCCAAT	(Berg <i>et al.</i> , 2011)
khh34	CATCGGAACCTATACTCTTTTAG	(Berg <i>et al.</i> , 2011)
khh36	TGAACCTCCAATAATAAATAAAAT	(Berg <i>et al.</i> , 2011)
<b>Primers used to create the <math>\Delta cbpD</math> amplicon</b>		
CbpD-1098	GTTGATTATCTTAGCAGCTCGT	Eldholm <i>et al.</i> , 2010)
CbpDR	CCAAGGGTTTGCTCGCAT	Eldholm <i>et al.</i> , 2010)
<b>Primers used to create <math>P_{comX-rodA}</math> in a <math>\Delta rodA</math> background</b>		
ds339	ATTTATATTTATTATTGGAGGTTCAATGAAACGTTCTCTCGACTCT AG	This work
ds340	ATTGGGAAGAGTTACATATTAGAAATTATTTAATTTGTTTTAATAC AACC	This work
ds342	AGAAAGTATTCGCTTTGAGTGC	This work
ds343	TCCAAAACCTGATCATTTCGATG	This work
css6	CACATTATCCATTA AAAATCAAAC TACTATTTATCAAAGTTCATTA AAAAATC	This work
css7	TTAAATGTGCTATAATACTAGAAAATACTTGGAGAAAATCATGGT AAAAGTAG	This work
css15	CTACTTTTACCATGATTTTCTCCTACTATTTATCAAAGTTC	This work
css16	TAATGAACTTTGATAAATAGTAGGAGAAAATCATGGTAAAAGTAG	This work
<b>Primers used to create <math>P_{comX-ftsW}</math> in a <math>\Delta ftsW</math> background</b>		
ds368	TTCCTCAATTCATAGAGTGTG	This work
ds369	ACAAGGCACGACGGTAAAGC	This work
css2	CACATTATCCATTA AAAATCAAAC AGTATCACC ACTCTACTAGG	This work
css3	TTAAATGTGCTATAATACTAGAAAATACTTGATAAAGAAAGGATA GTTTATGTC	This work
css9	TTTATATTTATTATTGGAGGTTCAATGAAGATTAGTAAGAGGCAC	This work
css10	GGGAAGAGTTACATATTAGAACTACTTCAACAGAAGGTTTCATTG	This work
css11	GACATAAACTATCCTTTCTTTATCAGTATCACC ACTCTACTAGG	This work
css12	CCTAGTAGAGTGGTGATACTGATAAAGAAAGGATAGTTTATGTC	This work
<b>Primers used to create the <math>\Delta pbp2a</math> amplicon</b>		
mts1.F	GCACAACCTGTTTCGTA CTCTTG	This work
mts2.R	CACATTATCCATTA AAAATCAAAC GC GTTTATTTTATCATCTTCAT C	This work
mts3.F	GTCCAAAAGCATAAAGGAAAGGATGCTTGTC AAAGCCTAGC	This work

mts4.R	AGGTTTACTTCTGCAACTGTG	This work
--------	-----------------------	-----------

---

**Primers used to create the *Δpbp1a* amplicon**

mts5.F	CCTGTGTTTCATAGCGAGG	This work
mts6.R	CACATTATCCATTAATAAAATCAAACCTTGTTTTACCACCTAATAAAAT G	This work
mts7.F	GTCCAAAAGCATAAGGAAAGCATTATCATCCAGATTTTTCTG	This work
mts8.R	AAAACGGCTTTGGTAGCAGATG	This work

---

**Primers used to create the *Δpbp1b* amplicon**

mts9.F	GCCTGTACTTGGTAGTTTGG	This work
mts10.R	CATTATCCATTAATAAAATCAAACGGATTTCTCACTTTATCTATTA	This work
mts11.F	GTCCAAAAGCATAAGGAAAGTTCTCTAAATGAAGTGGCCAATC	This work
mts12.R	GACTATTCCAGTATAGCAC	This work

---

**Primers used to create the *ΔstkP* amplicon**

khb410	AGAAATATTAGGTAGTGTGTTGTC	This work
khb411	CCAGACAGTCATGCCCAAATC	This work
gs321	AATTGCACATCTCAAATAACTACTCATTCTGCATCCTCCTCGT	This work
gs322	CGTCCAAAAGCATAAGGAAAGAAGCAGATGGATAATCAAATGA	This work

---

**Primers used to create the *ΔmapZ* amplicon**

ds239	TGCAGAAACACTATGCTCGC	This work
ds240	CACATTATCCATTAATAAAATCAAACGAGTATCCCTTTCTATTTTACC	This work
ds241	GTCCAAAAGCATAAGGAAAGGCAGTCGTTACAAAATTCTTTC	This work
ds242	TACCAGTTCCCTTGTTACCTG	This work

---

**Primers used to create the *Δpmp23* amplicon**

ds301	ATGATACCGAGCTGTCTTAG	This work
ds302	CACATTATCCATTAATAAAATCAAACCTATTTACTTTGGATATCCTCG A	This work
ds303	GTCCAAAAGCATAAGGAAAGACCAGGTGTTTTTGTATAAGTTTT C	This work
ds304	AAGGTTTTAGTGAAATCTGCATTG	This work

---

**Primers used to create the *P<sub>comX</sub>-mreC* and *ΔmreC* amplicons**

gs223	ATGGATAGTATGATTTTGGGG	This work
gs224	CTACGAGCTTGTTTTTCCAAC	This work
gs225	CACATTATCCATTAATAAAATCAAACATCCCTACCTTTATATCAAAA AC	This work
gs226	AAATACTTGTGGAGGTTCCATTAATTAGTGGGGAATTCATAATG	This work
gs227	ATTTATATTTATTATTCGAGGTTCAATGAACCGTTTTAAAAAATCA AAAT	This work
gs228	ATTGGGAAGAGTTACATATTAGAAATTATGAATTCCTCCACTAATT CTA	This work
gs229	ATCCCTACCTTTATATCAAAAAC	This work
gs230	GTTTTTGATATAAAGGTAGGGATAATTAGTGGGGAATTCATAATG	This work

---

**Primers used to create the *P<sub>comX</sub>-mreD* and *ΔmreD* amplicons**

gs231	GTCAATACCGACAATTGAAATG	This work
gs232	ACGGACAGGTGCTGCTGC	This work
gs233	CACATTATCCATTAATAAAATCAAACCTATGAATTCCTCCACTAATTCT A	This work
gs234	CGTCCAAAAGCATAAGGAAAGGAACGACATATAAATGTAACAAA	This work
gs235	TTATGAATTCCTCCACTAATTCTA	This work
gs236	TAGAATTAGTGGGGAATTCATAAGAACGACATATAAATGTAACAA A	This work

gs237	ATTTATATTTATTATTTCGAGGTTCAATGAGACAGTTGAAGCGAGTT	This work
gs238	ATTGGGAAGAGTTACATATTAGAAATTATAGATAATATTTTTCAA AAATAAAT	This work

---

**Primers used to create the  $\Delta rodZ$  amplicon**

khh445	TAGATTTACTTGATGAATTGGTAA	This work
khh446	CACATTATCCATTAATAAATCAAACACTTGTCCCTTCTTTCTAG	This work
khh447	TTAAATGTGCTATAATACTAGAAAATACTTGTGGAGTTCCATTGGAAAAACGAA TGAAAAAGAAC	This work
khh448	CCACACGTTGCTTTTGGCC	This work

---

**Primers used to create the  $\Delta gpsB$  amplicon**

gs301	CATCGGAATCGCACGTTTTTG	This work
gs302	CGTTTAAAGAGGCTAGACCC	This work
khh413	ATTTATATTTATTATTGGAGGTTCAATGGAGAGAGACATGGCAAG	This work
khh414	ATTGGGAAGAGTTACATATTAGAAATTAATAAATCTGAGTTATCTA AAATTT	This work
khh415	TTTAAATAACAGATTAATAAATAAATTATAAGTAGTTATTTGAGATGT GCAATT	This work
khh416	GTATTCAAATATATCCTCCTCACTCTCGCTTGCTAGTATTATTATA	This work

---

**Primers used to create  $P_{comX-spr0777}$  in a  $\Delta spr0777$  background**

khh480	ATTTATATTTATTATTGGAGGTTCAATGTTTCGTAGAAATAAATTA TTTT	This work
khh481	ATTGGGAAGAGTTACATATTAGAAATTACTTAGCTAATTCTCTTTC TC	This work
khh482	ACGATTTTGC GAAGTGTAATG	This work
khh483	CACATTATCCATTAATAAATCAAACGAGTTACCTCCCTCACTTTAT	This work
khh484	GTCCAAAAGCATAAGGAAAGAAGTCAGGAGAACCCTGATTT	This work
khh485	AAGGAATAATGGAGCCGGTG	This work

---

**Primers used to create  $P_{comX-ftsB}$  in a  $\Delta ftsB$  background**

ds293	ATTTACAAGAAAATTCGTCAAATTG	This work
ds294	CACATTATCCATTAATAAATCAAACCTTAGACATTTTCTTCTACCCGT G	This work
ds295	GTCCAAAAGCATAAGGAAAGTAAAATGGAAAATTTATTAGACGT A	This work
ds296	CAGTCGTATCTAACTGATAAAG	This work
ds297	TACGTCTAATAAATTTCCATTTTATTAGACATTTTCTTCTACCCGT G	This work
ds298	CACGGGTAGAAGAAAATGTCTAATAAAAATGGAAAATTTATTAGAC GTA	This work
ds299	ATTTATATTTATTATTGGAGGTTCAATGTCTAAAAATATTGTACAA TTGA	This work
ds300	ATTGGGAAGAGTTACATATTAGAAATCACCTTTGAAGCAAGTCAG G	This work

---

**Primers used to create  $P_{comX-murJ}$  in a  $\Delta murJ$  background**

khh392	GTTGAAGTTGCCAATGAGTTG	This work
khh393	CACATTATCCATTAATAAATCAAACAGATTCCTCATTCAATTTTGAT AA	This work
khh394	GTCCAAAAGCATAAGGAAAGGGTAGCATTTATAAATAAAAGGAA	This work
khh395	TTACGTTCCAGTGATTCTTGG	This work
khh396	ATTTATATTTATTATTGGAGGTTCAATGTCTGCACGAAAACAATCAC	This work
khh397	ATTGGGAAGAGTTACATATTAGAAATTACGAAAGCTTAAATTTTG CTC	This work

---

**Primers used to create  $P_{comX-mltG}$  in a  $\Delta mltG$  background**

ds355	CACATTATCCATTA AAAATCAAACAAGTTTTTCTCCTTGTTGATA A	This work
ds356	GTGCTATAATACTAGAAAATACTTACAACTAAAATTATGTGATA CTTC	This work
ds357	AAGTTTTTCTCCTTGTTGATAA	This work
ds358	TTATCAACAAGGAGGAAAACTTACAACTAAAATTATGTGATA TTC	This work
ds359	ATTTATATTTATTATTGGAGGTTCAATTGAGTGAAAAGTCAAGAGA AG	This work
ds360	ATTGGGAAGAGTTACATATTAGAAATTAGTTTAATTTGCTGTTGAC ATG	This work
ds361	AACTAGCCGCAGGTTGCTC	This work
ds362	AATTAAGATCATTCAAGCAAGC	This work
<b>Primers used to create <math>P_{comX}</math>-<i>spr1357</i> in a <math>\Delta</math><i>spr1357</i> background</b>		
khb496	ATTTATATTTATTATTGGAGGTTCAATGGAGCAAAAAGAGAAACA TTT	This work
khb497	ATTGGGAAGAGTTACATATTAGAACTATTGTTCACTCTTGACTTC C	This work
khb498	TCACGTGGAGTCTGACCATG	This work
khb499	CACATTATCCATTA AAAATCAAACAATACTTCCTTTCTATTGTTC TC	This work
khb500	GTCCAAAAGCATAAGGAAAGGTAGTCAGTGGTCTATATGAAT	This work
khb501	CTGGCTCCTCACTCTGCAA	This work
<b>Primers used to create the <math>\Delta</math><i>divIVA</i> amplicon</b>		
gs287	CCTGATTTTGGTAGCCTTCG	This work
gs288	CATAGTAAAGGGAAGTTGAAAC CACATTATCCATTA AAAATCAAACTCACTTACTTAATAATAACTG	This work
gs289	GAC	This work
gs290	CGTCCAAAAGCATAAGGAAAGCTCCAGTGCATCCGACAGG	This work
<b>Primers used to create the <i>divIVA</i><sub>T201A</sub> amplicon</b>		
ds204	GCACGTCAGTTCTCTCAAGCAG	This work
ds205	CTGCTTGAGAGAACTGACGTGCCATATCAATTGGTTCTTCTTCAA	This work
<b>Primers used to create the <i>divIVA</i><sub>T201E</sub> amplicon</b>		
ds208	GAACGTCAGTTCTCTCAAGCAG	This work
ds209	CTGCTTGAGAGAACTGACGTTCCATATCAATTGGTTCTTCTTCAA	This work
<b>Primers used to create the <i>divIVA</i><math>\Delta</math>40, <i>divIVA</i><math>\Delta</math>65, <i>divIVA</i><math>\Delta</math>74, <i>divIVA</i><math>\Delta</math>92 and <i>divIVA</i><math>\Delta</math>112 amplicons</b>		
dS226	CCTGTCGGATGCACTGGAGTTATTCTTTATCGGCTACCTCAATAC	This work
dS227	CCTGTCGGATGCACTGGAGTTATGGTTCTTCTTCAATTGGAGC	This work
dS245	CCTGTCGGATGCACTGGAGTTACGGTTCTCCAAGTACTTCG	This work
dS246	CCTGTCGGATGCACTGGAGTTAAAGATAAGTAGCTGTTGGACG	This work
dS247	CCTGTCGGATGCACTGGAGTTACTGACTCTCAATTGTAGATTTG	This work
<b>Primers used to create the <i>divIVA</i>-GFP, <i>divIVA</i><math>\Delta</math>92-GFP and <i>divIVA</i><math>\Delta</math>112-GFP amplicons</b>		
ds210	CTCTAGACTTCTGGTTCTTCATCTTCTGGTTCTTCATACATTG	This work
ds211	ATGAAGAACCAGAAGTCTAGAGGATCTGGTGGAGAAGCTGCAGC TAAAGCTGGAAGTATCAAACATCTTACCGGTTCTAAAGG	This work
ds212	CCTGTCGGATGCACTGGAGTTATGCGGCCGCTCCACTAG	This work
ds366	CTCTAGACTTCTGGTTCTTCATAAGATAAGTAGCTGTTGGAC	This work
ds367	CTCTAGACTTCTGGTTCTTCATCTGACTCTCAATTGTAGATTTG	This work
<b>Primers used to create T25 and T18 fusions of <i>pbp2b</i>, <i>mreD</i>, <i>divIVA</i>, <i>spr0777</i>, <i>rodA</i>, <i>pbp2x</i> and <i>spr1357</i> (restriction sites are underlined)</b>		
KHB426 Fwd <i>pbp2b</i>	TACGGGATCC <u>CAG</u> AAAATTTAACAGCCATTCGAT	This work

KHB427 Rev <i>pbp2b</i>	TACGGAATTCCTAATTCATTGGATGGTATTTTTG	This work
KHB428 Fwd <i>divIVA</i>	TACGAAGCTTGGTGAGGAATAGAATGCCAATT	This work
KHB453 Fwd <i>divIVA</i>	TACGGGATCCCAGGAATAGAATGCCAATTACATC	This work
KHB454 Rev <i>divIVA</i>	TACGGAATTCCTACTTCTGGTTCTTCATACAT	This work
GS.334 Rev <i>divIVA</i>	TACGGAATTCGACTTCTGGTTCTTCATACATTGG	This work
KHB462 Rev <i>rodA</i>	TACGGAATTCCTTATTTAATTTGTTTTAATACAACCT	This work
DS341 Fwd <i>rodA</i>	TACGGGATCCCAAACGTTCTCTCGACTCTAGAG	This work
KHB486 Fwd <i>pbp2x</i>	TACGTCTAGAG AAGTGGACAAAAAGAGTAATCC	This work
KHB487 Rev <i>pbp2x</i>	TACGGAATTCCTTAGTCTCCTAAAGTTAATGTAAT	This work
KHB505 Rev	TACGTGAATTCGATTGTTCACTCTTGACTTCCTC	This work
<i>spr1357</i>		
KHB506 Fwd	TACGACTCTAGAGATGGAGCAAAAAGAGAAACATTT	This work
<i>spr1357</i>		
GS.337 Fwd <i>spr0777</i>	GATCGGATCCCATGTTTCGTAGAAATAAATTATTTTT	This work
GS.338 Rev <i>spr0777</i>	GATCGAATTCGACTTAGCTAATTCTCTTTCTCGT	This work
GS.339 Rev <i>spr0777</i>	GATCGAATTCCTTACTTAGCTAATTCTCTTTCTC	This work
DS345 Fwd <i>mreD</i>	TACGTCTAGAGATGAGACAGTTGAAGCGAGTTG	This work
DS350 Rev <i>mreD</i>	TACGGAATTCGAGGTTCTCCTCCTCCACTTCCTCCTCCT CCTAGATAATATTTTTCAAAAATAAATTG	This work

968

969 Berg, K.H., Biørnstad, T.J., Straume, D., and Håvarstein, L.S. (2011) Peptide-regulated gene depletion

970 system developed for use in *Streptococcus pneumoniae*. J Bacteriol **193**: 5207-5215.

971

972 Eldholm, V., Johnsborg, O., Straume, D., Solheim Ohnstad, H., Berg, K.H., Hermoso, J.A., Håvarstein,

973 L.S. (2010) Pneumococcal CbpD is a murein hydrolase that requires a dual cell envelope binding

974 specificity to kill target cells during fratricide. Mol Microbiol **76**: 905-917

975

976 Johnsborg, O., Eldholm, V., Bjørnstad, M.L., and Håvarstein, L.S. (2008) A predatory mechanism

977 dramatically increases the efficiency of lateral gene transfer in *Streptococcus pneumoniae* and

978 related commensal species. Mol Microbiol **69**: 245-253.

979

980

981

982

983

984

985

986

987

988

989

990

991

992

993

994

995

996

997

998 **Table S2.** The peak area ratio between peak I and peak II in Fig. 4.

999

Strain	Gene deleted	Gene ectopically expressed	ComS <sup>1</sup> inducer ( $\mu$ M)	Peak I/Peak II		
				Exp. 1	Exp. 2	Average
RH1 <sup>2</sup>	NA <sup>3</sup>	NA	NA	2.7	2.4	2.6
SPH157	NA	<i>pbp2b</i>	2	3.3	3.1	3.2
SPH157	NA	<i>pbp2b</i>	0.02	2.1	2.2	2.2
SPH157	NA	<i>pbp2b</i>	0	0.8	0.8	0.8
SPH351	<i>mreD</i>	NA	NA	1.7	1.6	1.7
SPH354	NA	<i>rodA</i>	0.05	3.1	3.2	3.2
SPH354	NA	<i>rodA</i>	0	1.2	1.2	1.2
SPH355	NA	<i>spr0777</i>	0.2	2.2	2.1	2.2
SPH355	NA	<i>spr0777</i>	0	1.7	1.7	1.7
SPH361	<i>divIVA</i>	NA	NA	2.2	2.1	2.2

1000 <sup>1</sup> Depletion of target genes was performed by removing ComS from the medium (0  $\mu$ M ComS).  
 1001 A ComS concentration of 2  $\mu$ M induces the maximum rate of transcription from the P<sub>comX</sub>  
 1002 promoter. ComS concentrations of 0.02, 0.05 and 0.2  $\mu$ M was found to give wild-type-like  
 1003 morphologies and growth rates in the SPH157, SPH354 and SPH355 strains, respectively. <sup>2</sup>Wild-  
 1004 type strain. <sup>3</sup>Non applicable.

1005

1006

1007

1008

1009

1010

1011

1012

1013

1014

1015

1016

1017

1018

1019

1020

1021 **Table S3.** Plasmids used for BACTH analysis

Plasmids	Relevant characteristics	Reference
pKT25	For fusing the T25 domain at the N-terminus, Kan <sup>R</sup> .	Euromedex
pKNT25	For fusing the T25 domain at the C-terminus, Kan <sup>R</sup> .	Euromedex
pUT18C	For fusing the T18 domain at the N-terminus, Amp <sup>R</sup> .	Euromedex
pUT18	For fusing the T18 domain at the C-terminus, Amp <sup>R</sup> .	Euromedex
pKT25-zip	Expresses T25 fused to a leucine zipper domain, Kan <sup>R</sup> .	Euromedex
pUT18C-zip	Expresses T18 fused to a leucine zipper domain, Amp <sup>R</sup> .	Euromedex
pKT25-pbp2b	Expresses Pbp2b with the T25 domain fused at its N-terminus, Kan <sup>R</sup> .	This work
pUT18C-pbp2b	Expresses Pbp2b with the T18 domain fused at its N-terminus, Amp <sup>R</sup> .	This work
pKT25-pbp2x	Expresses Pbp2x with the T25 domain fused at its N-terminus, Kan <sup>R</sup> .	This work
pUT18C-rodA	Expresses RodA with the T18 domain fused at its N-terminus, Amp <sup>R</sup> .	This work
pUT18C-divIVA	Expresses DivIVA with the T18 domain fused at its N-terminus, Amp <sup>R</sup> .	This work
pUT18-divIVA	Expresses DivIVA with the T18 domain fused at its C-terminus, Amp <sup>R</sup> .	This work
pKNT25-divIVA	Expresses DivIVA with the T25 domain fused at its C-terminus, Kan <sup>R</sup> .	This work
pKT25-spr0777	Expresses Spr0777 with the T25 domain fused at its N-terminus, Kan <sup>R</sup> .	This work
pUT18-spr0777	Expresses Spr0777 with the T18 domain fused at its C-terminus, Amp <sup>R</sup> .	This work
pKNT25-mreD	Expresses MreD with the T25 domain fused at its C-terminus, Kan <sup>R</sup> .	This work
pUT18-spr1357	Expresses Spr1357 with the T25 domain fused at its C-terminus, Amp <sup>R</sup> .	This work

1022

1023

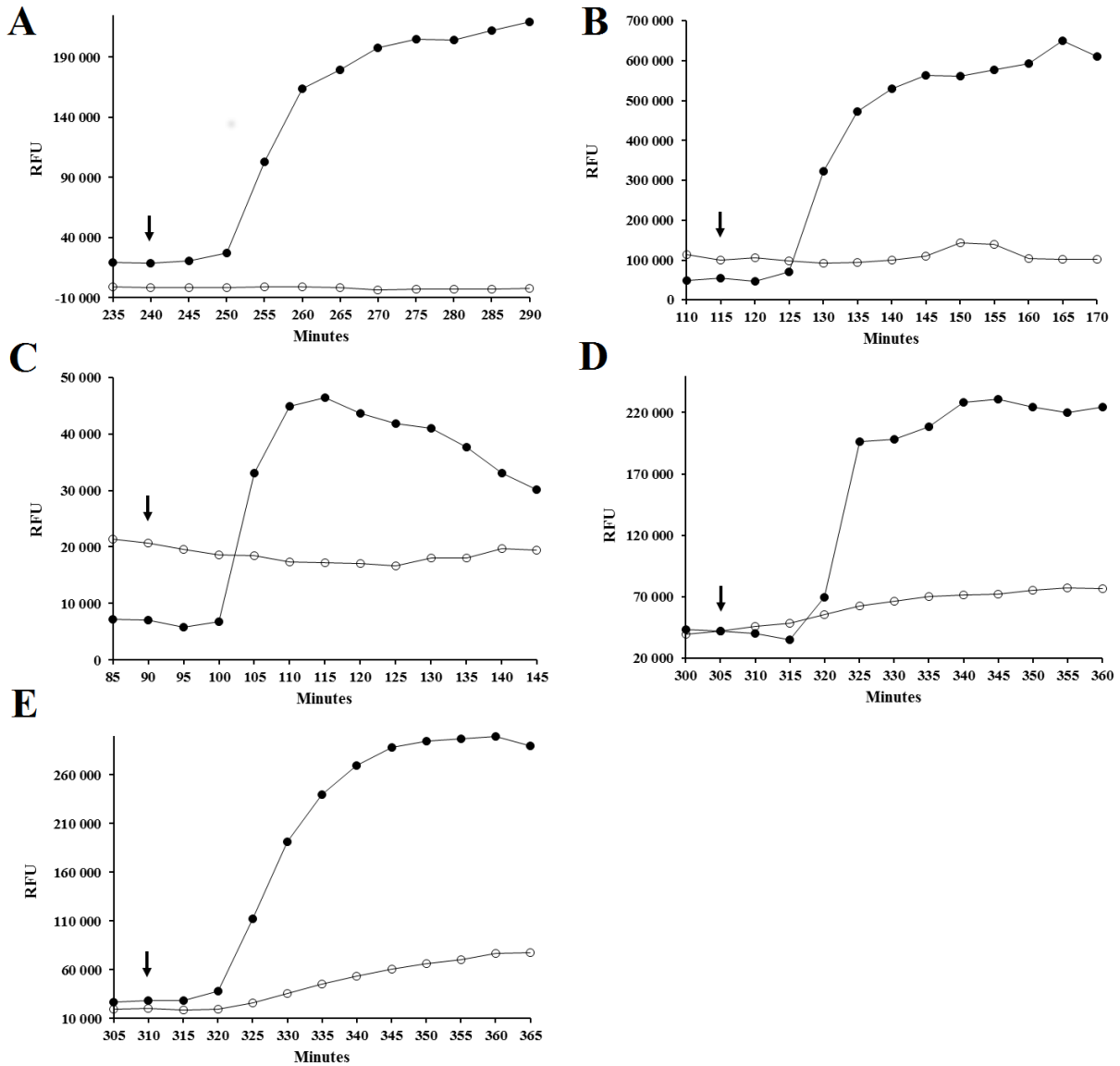
1024

1025

1026

1027

1028



1029

1030

1031

1032 **Fig. S1.** DNA-release assay demonstrating that competence induced autolysis in pneumococcal

1033 mutants deleted or depleted in PBP2b, MreD, RodA, DivIVA or Spr0777 is caused by CbpD.

1034 DNA release was measured in real time by culturing the cells in the presence of the membrane-

1035 impermeable Sytox Green Nucleic Acid Stain (Invitrogen™). Sytox Green fluoresces strongly

1036 upon binding DNA when excited at 485 nm. Competence was induced by addition of CSP (250

1037 ng ml<sup>-1</sup>) at the time points indicated by the arrows. The fluorescence was measured automatically

1038 every 5 min by a Synergy H1 Hybrid Reader. Results were expressed as relative fluorescence  
1039 units (RFU) and were normalized according to the number of cells at each time point. Solid  
1040 lines; *cbpD*<sup>+</sup> cultures. Dotted lines;  $\Delta$ *cbpD* cultures. Panel (a), strains SPH157<sup>CbpD<sup>+</sup></sup> and  
1041 SPH419 $\Delta$ *cbpD* (both depleted in PBP2b); panel (b), strains SPH351<sup>CbpD<sup>+</sup></sup> and SPH420 $\Delta$ *cbpD* (both  
1042  $\Delta$ *mreD*); panel (c), strains SPH361<sup>CbpD<sup>+</sup></sup> and SPH421 $\Delta$ *cbpD* (both  $\Delta$ *divIVA*); panel (d), strains  
1043 SPH354<sup>CbpD<sup>+</sup></sup> and SPH422 $\Delta$ *cbpD* (both depleted in RodA); panel (e), strains SPH355<sup>CbpD<sup>+</sup></sup> and  
1044 SPH423 $\Delta$ *cbpD* (both depleted in Spr0777).

1045

1046

1047

1048

1049

1050

1051

1052